IEEE Access
Multidisciplinary ⋮ Rapid Review ⋮ Open Access Journal

Received 10 October 2022, accepted 16 November 2022, date of publication 18 November 2022,
date of current version 23 November 2022.

Digital Object Identifier 10.1109/ACCESS.2022.3223443

TOPICAL REVIEW

Emerging Intelligent Bidirectional Charging Strategy Based on Recurrent Neural Network Accosting EMI and Temperature Effects for Electric Vehicle

SAIRAJ ARANDHAKAR[1], (Member, IEEE), NAKKA JAYARAM[1], YANNAM RAVI SHANKAR[2], GAURAV[1], (Student Member, IEEE), PULAVARTHI SATYA VENKATA KISHORE[3], (Student Member, IEEE), AND SUKANTA HALDER[4], (Member, IEEE)

[1]Department of Electrical Engineering, National Institute of Technology Andhra Pradesh, Tadepalligudem 534101, India
[2]School of Electrical and Computer Engineering, Dire Dawa University, Dire Dawa 1362, Ethiopia
[3]Department of Electrical and Electronics Engineering, Sri Vasavi Engineering College, Tadepalligudem 534101, India
[4]Department of Electrical Engineering, Sardar Vallabhbhai National Institute of Technology, Surat 395007, India

Corresponding author: Yannam Ravi Shankar (yannam.ravi@ddu.edu.et)

ABSTRACT Transportation is currently advancing towards Electric Vehicle (EV) technology. This paper presents a brief and systematic analysis of the real-time issues obtained in Electric Vehicles (EVs) due to the various ranges of energy storage devices. In general, EV energy management system is integrated with power electronic circuits for effective power conversion and reliable operation. Some issues are addressed while using the batteries in EV systems such as charging time, efficiency of battery, and raw materials. Not only battery issues but also real-time non-technical issues and operational issues are also discussed in this paper. During energy conversion with power electronic circuits, the system attains extreme temperature levels which in turn reduces the performance of the system. To maintain an optimum temperature level, it is important to study the temperature effect of the system at the most prior levels. Due to the adaption of power electronic components, some extent of noise is generated, technically treated as Electromagnetic Interference (EMI), as system capacity increases the EMI content also improved proportionately. Therefore, to mitigate the EMI effect, the low pass filter-based EMI filter is introduced in the system such that the noise level is suppressed. Bidirectional Charging System (BCS) is one of the emerging technologies in EV to obtain autonomous power supply systems in the form of Vehicle to Grid (V2G), Grid to Vehicle (G2V), and Vehicle to Load (V2L). To know the behaviour of BCS the proposed RNN controller is employed and is compared with ANN bidirectional charging model. BCS charging system with RNN controller has better dynamic response to exchange the power via DC/DC converter and AC/DC converter as compared to ANN controller.

INDEX TERMS Power electronic converter (PEC), electromagnetic compatibility (EMC), electric vehicle (EV), fuel cell electric vehicle (FCEV), EMI filter.

I. INTRODUCTION

Across the globe, most Internal Combustion (IC) engines are replaced with electric motors. Not only for the hike of fuel charges but also for the concern of the environment [1]. Vehicles powered by IC engines emit 20%-30% of greenhouse gas emissions. Additionally, there is a severe problem with fossil fuel depletion and growing awareness of deteriorating climate conditions has prompted the development of alternative energy sources [2]. Therefore, electric vehicles (EVs)

The associate editor coordinating the review of this manuscript and approving it for publication was Wenjie Feng.

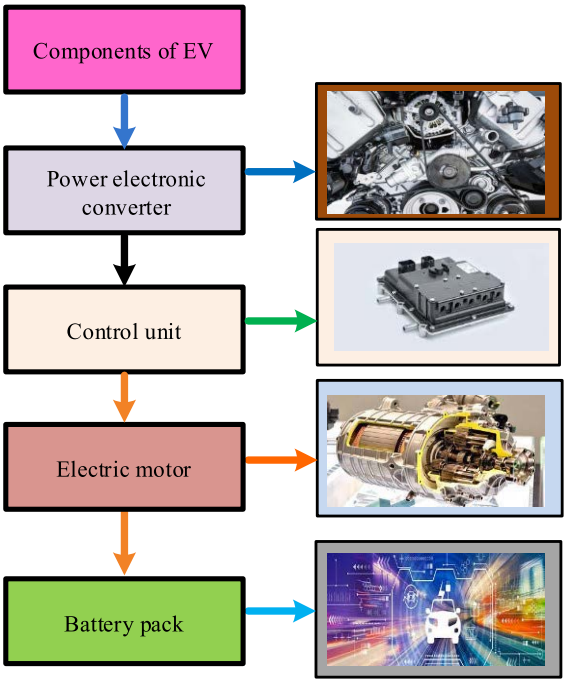

FIGURE 1. Basic Components of EV.

are suitable alternatives to replace combustion vehicles. EVs are not just a method of transportation, but also referred as new generation of electric equipment, allowing for clean and efficient transport [3], [7].

The EV architecture consists of power electronic converter, control unit, electric motor, and battery pack. EV is used as convenient load to stabilize the grid when there is significant proportion of fluctuating renewable energy supply [8]. The components of electric vehicles are shown in Fig.1. The specific EV design considerations are described as listed below [9].

1. Recognizing the EV environment and industry trends.
2. Evaluating the infrastructure needed for design, as well as integrating battery recycling.
3. Defining its power source for various scenarios such as production or reserve, standalone or hybrid.
4. Identifying the essential components of an electric vehicle propulsion system, such as single or multiple motors, converters, transmission systems, and installation methodologies.

In [10], developed an integrated controller for charging and driving the EVs. The controller permits the controller to concurrently accomplish motor drive and onboard charging for the vehicle. Authors used TMS320F28335-based experimental platform. A resistive load replicated the power battery to validate charging mode, and a 5 kW PMSM verified driving mode. Li et al. [11], examined the lifetime design of Plug-in hybrid electric vehicle, a hybrid electric vehicle like Battery electric vehicle batteries in domestic applications. The author experimented on second-use batteries based on residential load, and outdoor temperature. The quality of battery is tested for nearly 150Hours in software simulation and experimental ways.

In [12], developed a novel Game theory-based theoretical approach for congestion problem control. The authors used a sophisticated method of pricing, as well as the development of a plan to alleviate congestion in the network between Plug-in EVs and the utilized grid. Awami et al. [13], proposed the self-governing EV charge controller for mitigating the negative impacts during load fluctuations. Low-voltage nodes are more vulnerable to load variations than high-voltage nodes. The author addressed the estimation of load fluctuations depending upon the input provided to the EV source also considering various loading scenarios, distributed generators, system reconfiguration, and voltage control devices.

Zhao et al. [14], proposed the voltage-source converter for an onboard Electric Vehicle (EV) charger that is compatible with both single-phase and 3-phase grids. LCL filters are specifically designed to eliminate the harmonics absorbed by power converters. The author experimented on a 3KW prototype. The harmonics are reduced by transforming the source from star to delta pattern. Therefore, effective utilization of DC link voltage and filter capacity increases. Park et al. [15], implemented the estimated controller and applied it to the battery cooling controller for an electric vehicle. The battery life is degraded when the battery temperature is too low or high, so the author developed the above controller in proper stochastic prediction manner [16]. The proposed controller has robust performance as compared with other thermal management controllers.

Naseri et al. [17], proposed the regenerative braking system in EVs based on the balancing features of batteries and supercapacitors. Brush Less DC (BLDC) motor acts as a generator during the braking operation. The EV configuration is associated with hybrid energy storage systems, so the appropriate switching operation is performed i.e., the effective energy is transferred between super capacitor and battery through inverter. An Artificial Neural Network (ANN) is used to balance the braking force. PI controller adjusts the brake current at the same time for constant torque braking.

Fu et al. [18], proposed an output voltage control with harmonic correction and a virtual impedance term to achieve high power quality and sufficient damping for the EV. To achieve proper evaluation, the author introduced the time delay for the controller. The efficiency of the design process is validated by simulation results and experimental data on an EV battery charger prototype comprised of silicon carbide devices that includes one voltage source inverter and one isolated DC/DC converter.

In [19], developed a battery based on ultracapacitor hybrid energy storage system for the rippled load. Ultracapacitor energy storage is clearly understood by using the MATLAB/Simulink platform, after examining all the results the authors decided that the energy storage capacity of developed method is effective as compared to Lead-acid storage battery.

Stirban et al. [20], introduced a Current and frequency-based sensor less control technique for a 3-phase, 4 pole permanent magnet BLDC motor. By considering the prediction of a line-to-line permanent magnetic flux linkage, the control strategy investigation using a real-time offline finite element technique based on supported position and speed observer. A digital system is used to represent the simulation process.

Mishra et al. [21], investigated a sigma-modified power control and gain adaptive implementation for EV charging applications. Sigma-mod control is effective for the analysis of a wide range of supply voltage distortion. Lyapunov candidate analytic function is used for convergence checking process. The author successfully demonstrated the gain of adaptive control through experimental validation.

In [22], developed a novel hybrid forecasting model for electric vehicle fleet charging that is based on numerous decompositions. The Swarm Decomposition, often known as SWD, is included in the Complete Ensemble Empirical Mode Decomposition Adaptive Noise (CEEMDAN) method through the utilization of the presented strategy. Authors compared both traditional and hybrid models and concluded as the developed model performed significantly better.

Baszynski et al. [23], implemented a digital algorithm in a Field Programmable Gate Array (FPGA) approach for monitoring the high-speed functioning of a BLDC motor using the PI control mechanism. The proposed method frequency of measurement is six for two pole motor and twelve for four pole motor. The FPGA measuring system is highly efficient, and there is no need to use any additional external devices for high-speed measurements, such as sensors and tachometers, etc., which decreases the cost of BLDC motor production.

Electromagnetic (EM) field interferes with power electronic equipment, which happens when the electronic device is near the EM field and causes interference in the radio frequency band. Electric vehicle has power electronic devices, which results in developing EMI issues. These issues are clearly addressed in Table 1. This paper is organized as the real-time issues of advanced automobile technology based on Electric Vehicles (EVs). Section II described generally real-time issues in EV. The drive mechanism of EV based on Power electronic converters is depicted in Section III. The influence of various parameters to change the performance of EV is prescribed in the form of technical issues, which are reported in Section IV. Section V, concludes the main reviews/ findings of this paper.

II. MODELING OF EV

The basic dynamics of a conventional vehicle are used for the formulation of an electric vehicle. In EV traction power is supplied to the electric motor using battery as shown in Fig.2. The traction motor generates torque, which causes the power train to move. The clutch, gearbox, differential, and driveshaft comprise the EV power train transmission. Power electronic converters are helped to control the speed and torque of the motor. The auxiliary loads are incorporated with systems for comfort, lighting, and safety. Maximum voltage of the battery is checked by using braking resistor during regenerative braking [42]. From the figure, thick lines represent the high voltage DC bus and dotted lines represented the low voltage DC bus.

A. DYNAMIC EV MODEL

To know the behaviour of EV is mathematically expressed by applying the fundamental dynamic and rotational physics, especially the concepts of Newton's Law of Motion [43]. The forces acting on the vehicle body represent the state of EV as depicted in Fig. 3. Vehicle has mass m moving with a velocity ($\overrightarrow{V}$), then the equation of motion is obtained as

$$m\frac{d\overrightarrow{V}}{dt} = (\overrightarrow{F_{tF}} + \overrightarrow{F_{tR}}) - (\overrightarrow{F_{rR}} + \overrightarrow{F_{rF}} + \overrightarrow{F_u} + \overrightarrow{F_g}) \quad (1)$$

Vehicle bodies are influenced by external forces, which are forward tractive force $\overrightarrow{F_t}$ rolling resistance moment $\overrightarrow{F_r}$, aerodynamic drag $\overrightarrow{F_u}$, grading resistance $\overrightarrow{F_g}$ tractive forces of front and rear wheels are represented as $\overrightarrow{F_{tF}}$ and $\overrightarrow{F_{tR}}$, vehicle velocity is positive when the vehicle is in forward direction. When the vehicle's velocity is reversed, the result is negative. Rolling reaction force is expressed as

$$\overrightarrow{F_r} = mgf_r \cos\alpha \cdot \frac{\overrightarrow{V}}{|V|} \quad (2)$$

where f_r is the coefficient of rolling resistance coefficient, α denotes the road angle in radians, and g is the acceleration due to gravity. Aerodynamic drag is acted upon the vehicle, vehicle velocity $\overrightarrow{V}$, vehicle anterior area A_f, air density ρ, and force due to wind $\overrightarrow{F_W}$ is expressed as

$$\overrightarrow{F_W} = \frac{1}{2}\rho A_f C_d \left(\overrightarrow{V} + \overrightarrow{V_W}\right)^2 \cdot \frac{\left(\overrightarrow{V + V_W}\right)}{|V + V_W|} \quad (3)$$

Velocity of wind (V_W), Aerodynamic drag coefficient (C_d). Maximum extent of dragging force (F_{tmax}) is required to maintain the pulling force (W), and the road adherence coefficient is denoted as μ. The maximum tractive effort obtained as

$$F_{t\max} = \mu \cdot W \quad (4)$$

The downward opposing tractive force with grading resistance is given as

$$\overrightarrow{F_r} = mg\sin\alpha \quad (5)$$

The resultant force obtained from the load acting on the front and rear wheels (W_F, W_R) can be given as

$$\overrightarrow{W_F} = \frac{L_B}{L}m_g\cos\alpha - \frac{h_g}{L}\left[\overrightarrow{F_t} - \overrightarrow{F_R}\left(1 - \frac{r_d Y}{h_g}\right)\right] \quad (6)$$

$$\overrightarrow{W_R} = \frac{L_A}{L}m_g\cos\alpha - \frac{h_g}{L}\left[\overrightarrow{F_t} - \overrightarrow{F_R}\left(1 - \frac{r_d Y}{h_g}\right)\right] \quad (7)$$

TABLE 1. Mitigation EMI techniques in various ranges of EVS.

S.NO	Author Details	Voltage Rating	Control Techniques	Addressed Issues	Advantages	Disadvantages
1	Guido Ala *et al.* (2007) [24]	42V	Finite-Difference Time –Domain (FDTD)	a) Electro Magnetic Compatibility (EMC) b) On board Electro Magnetic Interference c) Open boundary problems during Electro Magnetic emissions	a) Requires only current measurement b) Open boundary problems can be eliminated using Absorbing Boundary Conditions (ABCs).	a) Does not measure the radiated emissions b) Expensive measurement setup
2	Huang Xiaoliang *et al.* (2013) [25]	72V	Frequency varying filter technique	a) Energy storage capacity of Super Capacitors (SC) b) Energy Management between two power banks (Battery and SC)	a) Easy power control b) The optimized interface between SC and Half Controlled Converter (HCC).	Usage of only HCC so operated only at a limited extent
3	Battiston *et al.* (2016) [26]	110V	Improved Control Technique based on Flatness property	a) Stability and Control issues b) Effect of system non-linearity and the control strategy	a) Stability, robustness, and reduction in size of the Quasi Z-source inverter b) Favorable for Transport application due to less weight, volume c) Less Expensive	Using only one loop control in the operation
4	Zhen Zhang *et al.* (2016) [27]	220V	Pulse Width Modulation (PWM) method	a) Power quality issues in Vehicle to Grid connected system (V2G) b) EMI c) Problems Associated with switching signal	a) Cooperative to the smart grid system by providing proper electromagnetic signals. b) EMI and EMC-based noises are filtered out. c) Reduces the implementation complexity. d) Independent of any external control methods e) A sufficient amount of battery energy is utilized for mitigation of EMI.	Compromising the output voltage.
5	Djilali Hamza *et al.* (2013) [28]	235V	Digital Active EMI Filter (DAEF)	a) EMI, EMC b) Interfacing issues between Digital Signal Processing (DSP) and power converter	a) Flexible power conversion b) Greatly reduces the size and weight of the system. c) Reduces the overall cost of the system.	Limited amount of controlling during system integration.
6	Juuso Lindgren *et al.* (2016) [29]	250V	Hybrid Artificial Neural Network (HANN)	a) Temperature-based trip failure b) Power failure issues c) Effect of internal resistance in the charging phenomena	a) Effective Battery Thermal Management (EBTM) b) Efficiency is maximized even at the optimal battery temperature.	Heating issues occurred during the operation.
7	Robert Alvarez *et al.* (2012) [30]	288V	Low ambient temperature emissions are measured using a Chassis dynamometer	a) Fuel consumption and CO_2 emissions b) Low ambient temperature on HEV c) Compared the issues in Electrochemical process with EV	a) Regulated pollutants of HEVs are reduced by 30% to 85%. b) Increases fuel saving by reducing emissions.	Observed only in hot phase driving conditions.
8	Di Han *et al.* (2016) [31]	100V	Case study on common mode EMI	a) EMI and EMC emissions. b) Common mode noise spectrum and vibration in voltage transition rates.	a) Gallium Nitride High Electron Mobility Transistor (GaN HEMT) switching speed is high as compared to Si MOSFET. b) Converter efficiency and CM noise are eliminated.	Complex design

TABLE 1. *(Continued.)* **Mitigation EMI techniques in various ranges of EVS.**

9	Pengwei Sun *et al.* (2012) [32]	300V	Soft Switching method	a) Switching losses b) Conduction loss	Switching losses are eliminated using the soft switching modules across the inverter.	As the increase in temperature reduced the efficiency
10	Seok-Hyun Yu *et al.* (2017) [33]	254V	Heat Source analysis	a) Heating issues b) Skin Effect c) Losses associated with induction heater. d) Harmonics are present in the heater.	a) Effective thermal management b) Reduce the harmonics using Control algorithm	Reduces the Robustness due to high amount of heat.
11	Zheng Wang *et al.* (2019) [34]	350V	EV integrated power conversion system using a small film capacitor	a) Power conversion issues. b) Switching losses c) Control schemes	a) Effective switching states obtained after adding the small capacitor is connected to the DC link. b) Effective power conversion system.	Lack of information regarding harmonics.
12	Yun Zhang *et al.* (2017) [35]	300V	Switched capacitor bidirectional DC-DC converter	a) Voltage stress during the conversion b) Interfacing issues	a) Satisfies the dynamic response complexity. b) Protecting the battery from instantaneous changes in the current.	Power conversion during transient conditions is not much better as compared to a step change.
13	Yousu Yao *et al.* (2020) [36]	100V	Parameter optimization method	a) Ripples in the current waveform. b) Signal issues regarding interface between transmitter and receiver.	a) Achieved the wireless charging system in EV using Boost Converter. b) Current ripples are minimized.	High efficiency is achieved only at less distance.
14	Ahmed Sheir *et al.* (2018) [37]	200V	Modified the configuration of bi-directional inverter	Fluctuation of voltage and current during the faulty condition.	a) Size and weight of the converter is reduced by 20%. b) Mutual balance between capacitor and power switches. c) Capacity of the conversion system is improved.	Lack of information regarding lower range of EVs.
15	Lea Dorn-Gomba *et al.* (2017) [38]	150V	Multi-source inverter topology	a) Braking operation b) Conversion and interfacing issues	c) Gives the proper range of voltages to the load. d) Increases the efficiency of traction devices	Operating modes are studied only with inverter circuit
16	Ruoyun Shi *et al.* (2017) [39]	380V	Dual Inverter Drive (DID)	a) Charging and Discharging issues b) Harmonic analysis	a) Fast charging b) Effective energy balancing c) Integration requires less cost	Using with simple uncontrolled rectifier can restrict the power flow.
17	Yang Han *et al.* (2018) [40]	200V	High-speed switching operation using Silicon Carbide devices	a) Switching losses b) Adjustment of voltage levels at the output	a) Reliability of the system b) Increases the switching speed with fewer amounts of losses. c) Better performance.	a) Complete losses are not eliminated. b) High sensitive to the change in load
18	Zhong Du *et al.* (2009) [41]	100V	Cascaded H-bridge Multi-level Inverter	a) Issues in unequal phase voltage distribution b) Cascading operation	a) Size and weight of the system reduce due to lack of inductors in the HEV converter. b) Achieved a robust switching scheme.	Harmonics are limited up to a certain extent.

where, corresponding lengths and heights are L_a, L_b, L, h_g fluctuating resistance r_d Y of the tire is shown in Fig.3.

After examining the traction force of various types of roads, results that the sliding of the vehicle-driven wheel is

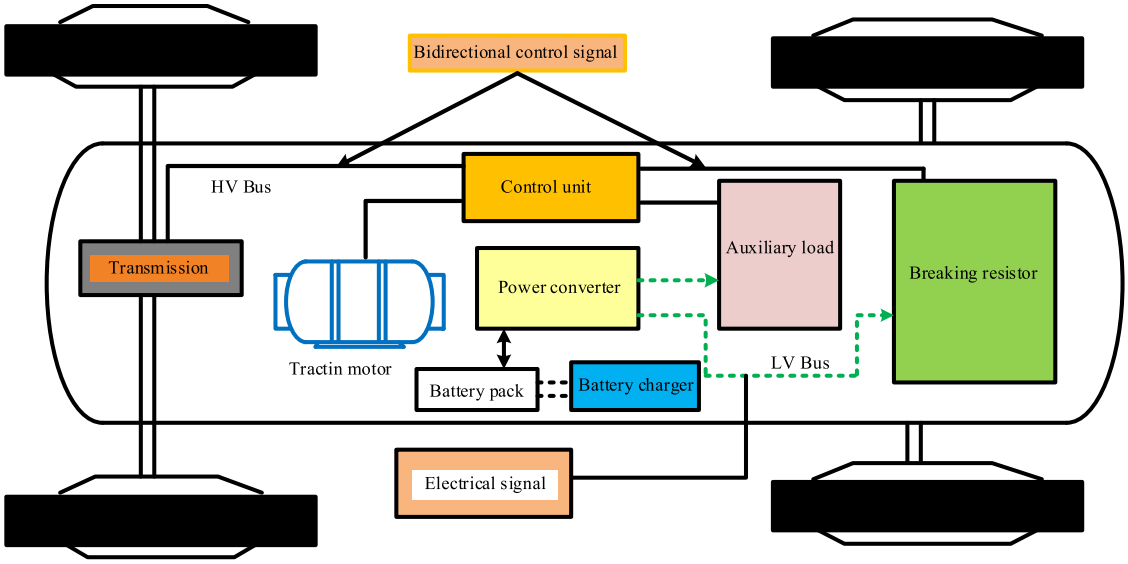

FIGURE 2. Electric Vehicle power train.

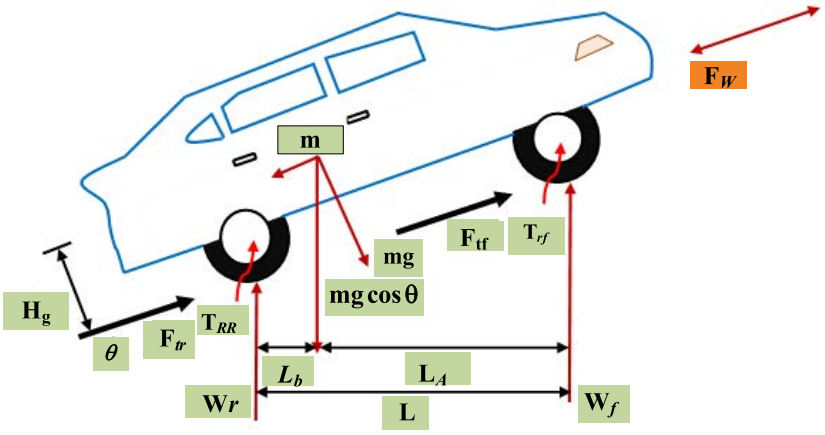

FIGURE 3. Dynamic Forces acting on the EV.

crucial for the drive wheel. Frictional movement between wheels and surface is

$$S_D = \left(1 - \frac{V_t}{r \cdot \omega}\right) \times 100\%8 \tag{8a}$$

$$S_D = \left(1 - \frac{r_e}{r}\right) \times 100\%8 \tag{8b}$$

$$S_B = \left(1 - \frac{r \cdot \omega}{V_t}\right) \times 100\%8 \tag{8c}$$

$$S_B = \left(1 - \frac{r}{r_e}\right) \times 100\%8 \tag{8d}$$

The above equations represent the driver slip (S_D), Braking slip (S_B), speed translation at the centre of the tire (V_t), angular speed (ω) of the tire, rolling radius (r), and effective radius (r_e) indicate the above Eq. 8(a)-8(d).

B. FOUR-WHEEL PLANAR DYNAMIC MODEL

The uphill motion of the kinematic model is discussed in previous section. The horizontal or planar road, during control design problems [44]. The longitudinal, lateral, and vertical movements of the vehicle's centre of gravity are defined by x, y, and z. The yaw and rolling angles are represented by ϕ_Y and ϕ_R. According to Newton's law of motion the longitudinal and lateral accelerations (a_X, a_Y) are formulated as

$$a_X = \frac{1}{m}\left(U_1 - U_2 + F_{X,3} + F_{X,4}\right) \tag{9}$$

$$\left.\begin{aligned} U_1 &= F_{X,1}\cos\delta_1 + F_{X,2}\cos\delta_2 \\ U_2 &= F_{Y,1}\sin\delta_1 + F_{Y,2}\sin\delta_2 \end{aligned}\right\} \tag{10}$$

$$a_Y = \frac{1}{m}\left(S_1 - S_2 + F_{Y,3} + F_{Y,4}\right) \tag{11}$$

$$\left.\begin{aligned} S_1 &= F_{X,1}\sin\delta_1 + F_{X,2}\sin\delta_2 \\ S_2 &= F_{Y,1}\cos\delta_1 + F_{Y,2}\cos\delta_2 \end{aligned}\right\} \tag{12}$$

Newton's law-based yaw speed on the initial instant is calculated as

$$\left.\begin{aligned} I(\varphi_R) = {} & L_A(F_{Y,1}\cos\delta_1 + F_{Y,2}\cos\delta_2 + F_{X,1}\sin\delta_1 + \\ & F_{X,2}\sin\delta_2) - L_B(F_{Y,3} + F_{Y,4}) + W_F(F_{Y,1}\sin\delta_1 \\ & -F_{Y,2}\sin\delta_2 - F_{X,1}\cos\delta_1 + F_{X,2}\cos\delta_2) + \\ & W_F(F_{X,3} + F_{X,4}) \end{aligned}\right\} \tag{13}$$

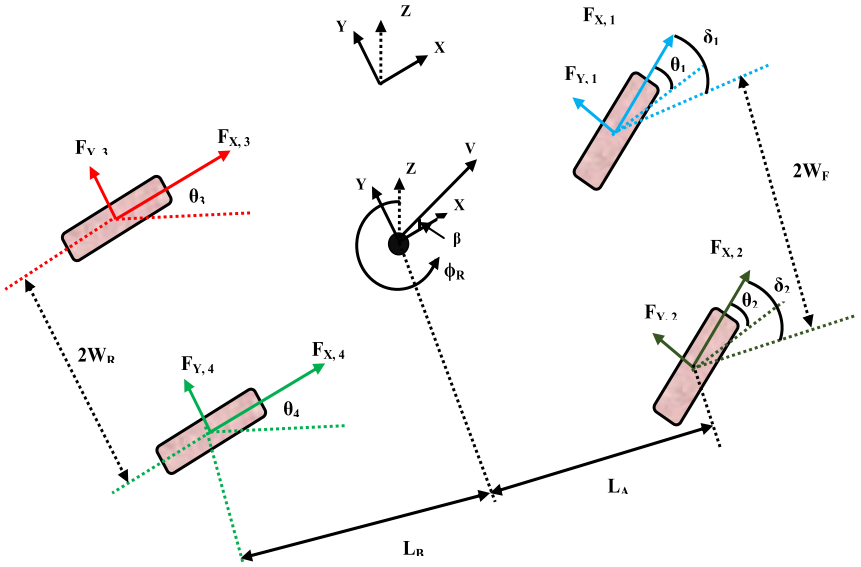

FIGURE 4. Kinematic model of a four-wheel planar structure.

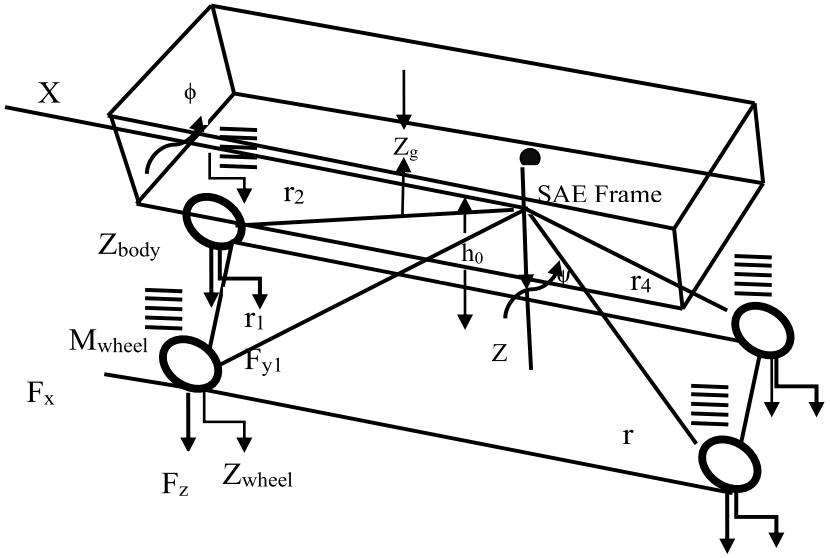

FIGURE 5. SAE frame of reference and vehicle model.

Fig.4 depicts the dimensions of the vehicle L_A, L_B, W_F, and W_R. The slip angle (β) is obtained based on the kinematics and geometry of vehicle body. At the centre of gravity, the translational speed is described w.r.t centre of each wheel using Eq. (14)-(17).

$$V_{t1} = (V_X - W_F\varphi_Y)\cos\delta_1 + (V_Y + L_A\varphi_Y)\sin\delta_1 \quad (14)$$

$$V_{t2} = (V_X - W_F\varphi_Y)\cos\delta_2 + (V_Y + L_A\varphi_Y)\sin\delta_2 \quad (15)$$

$$V_{t3} = (V_X - W_F\varphi_Y) \quad (16)$$

$$V_{t4} = (V_X + W_F\varphi_Y) \quad (17)$$

C. MULTIBODY DYNAMIC MODEL

The multi-body dynamic model from Fig.5 represents various subsystem features of the couplings in the vehicle, as well as many kinematic and non-linear constraints [45]. Differential equations describing the motion of the vehicle and the applied forces, such as bushing reactions and tire forces are found to capitulate the system position variables and the Lagrange model for the joint's reactions. These equations are developed using a genetic method based on the constrained system Lagrange's equations. Legrangeous multiplier (λ), coordinate vector (q), the matrix equation is given as

$$[J](q,\lambda)^T = F_q \quad (18)$$

where,

$$J = \begin{pmatrix} \frac{S}{dt}\frac{\partial K}{\partial q} + \frac{\partial K}{\partial q} & \frac{\partial C}{\partial \lambda} \\ \frac{\partial C}{\partial q} & 0 \end{pmatrix} \quad (19)$$

III. TECHNICAL AND NON-TECHNICAL IMPACTS OF EV

Even after producing an environmentally friendly product, this industry continues to face several barriers which are depicted in Fig. 6.

A. POLICY IMPACTS

1) ELECTRIC TARIFF POLICIES

The infrastructure for EV charging to hasten the electric vehicle revolution. The energy experts stated that there are no operating license requirements for EV charging stations worldwide, which might aid in the development of a larger global network of EV charging stations. The government offers discounts to buyers of EVs, lowers the applicable rate of taxes on Li-ion batteries, and offers incentives to the public transit sector to switch to electric cars [46].

2) DEMAND RESPONSE

To ensure that all customers have access to power during times of peak energy demand, utilities may better control the electrical grid with the use of demand response (DR) and load management technologies. Although it occasionally also refers to changeable pricing based on demand, the phrase ''demand response'' is most often used to explain reducing power to certain equipment.

B. INFRASTRUCTURE ISSUES

1) BATTERY REPROCESSING

Although electric car batteries are made to last for a certain period, they will eventually degrade. Manufacturers do not disclose actual pricing for battery replacement nevertheless, if replacement is necessary after the warranty has expired, the price will rise since a new battery must be purchased. Batteries' chemical components, including lithium, nickel, cobalt, manganese, and titanium, not only increase the efficiency of the supply chain but also pose a threat to the environment [47].

2) CHARGING INFRASTRUCTURE

Based on a design perspective, EV manufacturers recognized the Chargeable batteries, so that discharge batteries can be replaced with fully charged ones. The Charging station can arrange to charge their batteries at off-peak hours when the power tariff is lower [48].

C. MARKETING ISSUES

1) HIGH CAPITAL COST

Electric vehicle battery packs are costly, and they are replaced by many times throughout their lifespan. When compared to electric automobiles, gas-powered automobiles are less expensive [49].

2) CONSUMER PERCEPTION

Consumer reputation is critical in acquiring qualified customers and maintaining existing models. Although the increasing variety of electrical vehicles, the selection of importing an EV leftover controlled and is predictable to remain in the future. According to studies, lack of awareness, financial benefits, and knowledge of vehicular technology contains a direct impact on the approval of EVs [50].

3) RAW MATERIALS FOR THE BATTERIES

EV batteries consist of Lithium (Li), nickel (Ni), phosphate (P), and manganese (Mn), along with graphite (Gr) and cobalt (Co). To filter destructive gases, catalyzers for ignition cars need platinum, rhodium, and palladium. Lithium-ion batteries alone need 7 million tons of Ni per year, which leads to an increase in lithium and cobalt use from 15–22 times [51].

4) VEHICLE SERVICING

To secure the EV, an expert is necessary to repair, troubleshoot and preserve it. They are able to use their expertise to solve the problem as soon as feasible.

D. CLASSIFICATION OF EV

The EVs provide convenient features like noise less travel, availability of required torque, less energy utilization, and preservation price minimum, thus all features are much attracted to the automobile industry to switch towards EVs. All the above-mentioned qualities are much better than IC engine-based vehicles [52]. EVs are mainly classified into two types, one is autonomous EVs (AEV) and another one is Plug-in Electric Vehicles (PEV). The classification of EV is represented as shown in Fig.7.

1) FUEL CELL ELECTRIC VEHICLE (FCEV)

FCEV layout is the same as the BEVs exchanging batteries with a hydrogen (H_2) fuel arrangement depicted in Fig.7. In FCEVs, hydrogen is used as a fuel, and batteries are used as sole source of energy. The fuel cell, which converts hydrogen to electric energy, provides the electric energy required for vehicle propulsion. In FCEVs, the proton exchange membrane is a sophisticated model. Additionally, the nil notions are largely practical for FCEVs. Because the technology is still in its infancy, hydrogen fuel is expensive, and fueling the car is a laborious process [53].

2) FUSION/HYBRID ELECTRICAL VEHICLE (HEV)

To increase the driving range of BEVs, HEVs are created by fusing an ICE and an EV power train. The main parts of an HEV are the ICE, electric motor battery, fuel tank, and control system [54]. The classification of HEV is depicted in Fig.7. This assembly has three parts

i. **Driveshaft:** This device mechanically connects the electric drivetrain to the ICE supply.
ii. **Energy storage systems (ESS):** Maintain the flow of electricity from sources to loads. To extend battery life cycles and meet transient load requirements, a battery with an ultra-capacitor is attached.

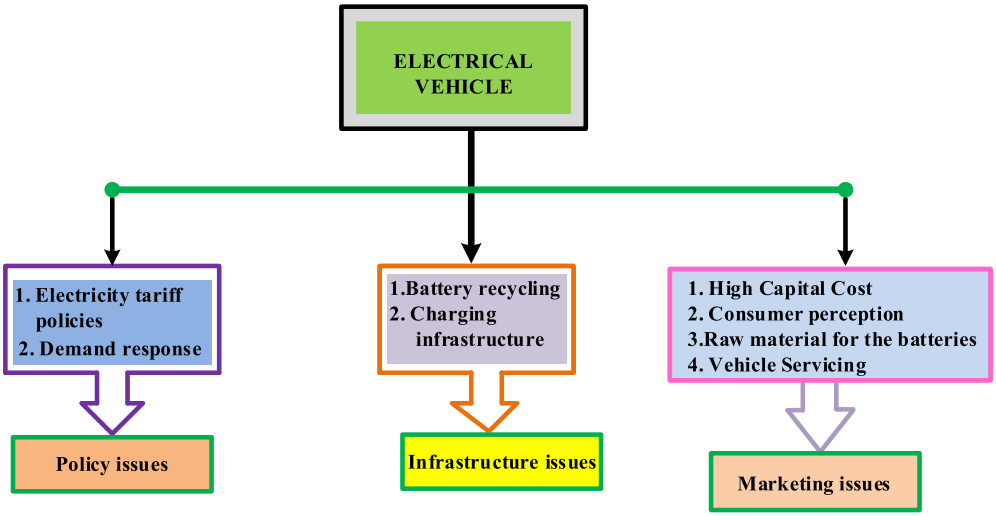

FIGURE 6. Policy, Infrastructure and Marketing Issues of EV.

iii. **Control system:** Oversees the electric drivetrain and internal combustion engine while effectively optimizing energy storage systems.

3) BATTERY ELECTRIC VEHICLE (BEV)

A battery serves as the only energy source used for vehicle propulsion in a BEV, or pure electric vehicle. BEVs are powered by huge battery packs that emit no pollutants. The battery is charged through an external outlet or the grid. Motors with high torque are used in BEVs to provide the needed torque, resulting in a loss in powertrain performance. loss in mechanical transmission and vehicle weight is quite low. The architecture is fairly basic, with a restricted driving range that is determined by the battery pack. These are ideal for short-distance city journeys with frequent halt driving patterns [55].

4) PLUG IN HYBRID ELECTRIC VEHICLE (PHEV)

PHEVs have the same design as HEVs, excluding high-efficiency onboard battery packs (see Fig. 8). Driving range adapters are another name for PHEV devices. Charge depletion mode is used in PHEVs until the current battery SOC limit was reached After that, leave the vehicle in charge maintaining mode until it is fully charged. The combination of charge depletion and sustaining modes leads to more complicated control methods as compared to HEVs. PHEVs produce less pollution and use less fuel than HEVs [56].

E. POWER ELECTRONIC DRIVER

Inside an electric propulsion system, power electronic devices are the most important components for improving system efficiency, a power switching device with closed-loop control and a switching strategy is used. The switching operation of thyristors is replaced with new power devices such as bipolar junction transistors (BJT), metal oxide semiconductor field effect transistors (MOSFET), gate turn-off thyristors (GTO), and insulated gate bipolar transistors (IGBT). For electric propulsion vehicles, there are three main types of semiconductor devices often employed [57], [60]. After examining the properties of all power devices, IGBTs are gaining attention for use in electric vehicles. IGBTs have several benefits over other devices, including higher BJTs having excellent conductivity and high-power density, as well as great efficiency, compactness, and a cheap cost of useable power. Each module has six thyristors, and the driving circuit is included inside the same package [61].

F. RELIABILITY OF POWER ELECTRONICS

The fundamental enabler is power electronics technology to improve EV/HEV self-sustained technology in the form of drives. Different power levels and voltage levels i.e., 12V and 450 V are involved in EV/HEV conversion. Therefore, excellent reliability of power electronic components is essential for EV/HEV applications to meet the expected acceptable failure rate, operational behaviour, and safety levels [62]. The reliability of the power electronic converter is depicted in Fig.8. The important power electronic sources used in EVs are DC-DC converters, Rectifiers, and Inverters. In the case of PEVs used in residential settings, the grid voltage that is taken through the plug is either 110V/60Hz or 220V/50Hz. single-phase ac input.

G. CHARGING TIME

The driving range is a problem that is strongly related to the difficulty of charging time. The EV can take up to 8 hours to completely charge from nothing using a 7 kW charging station and a slow charger [63]. The duration of time required to charge the battery is mostly influenced by its size. In addition,

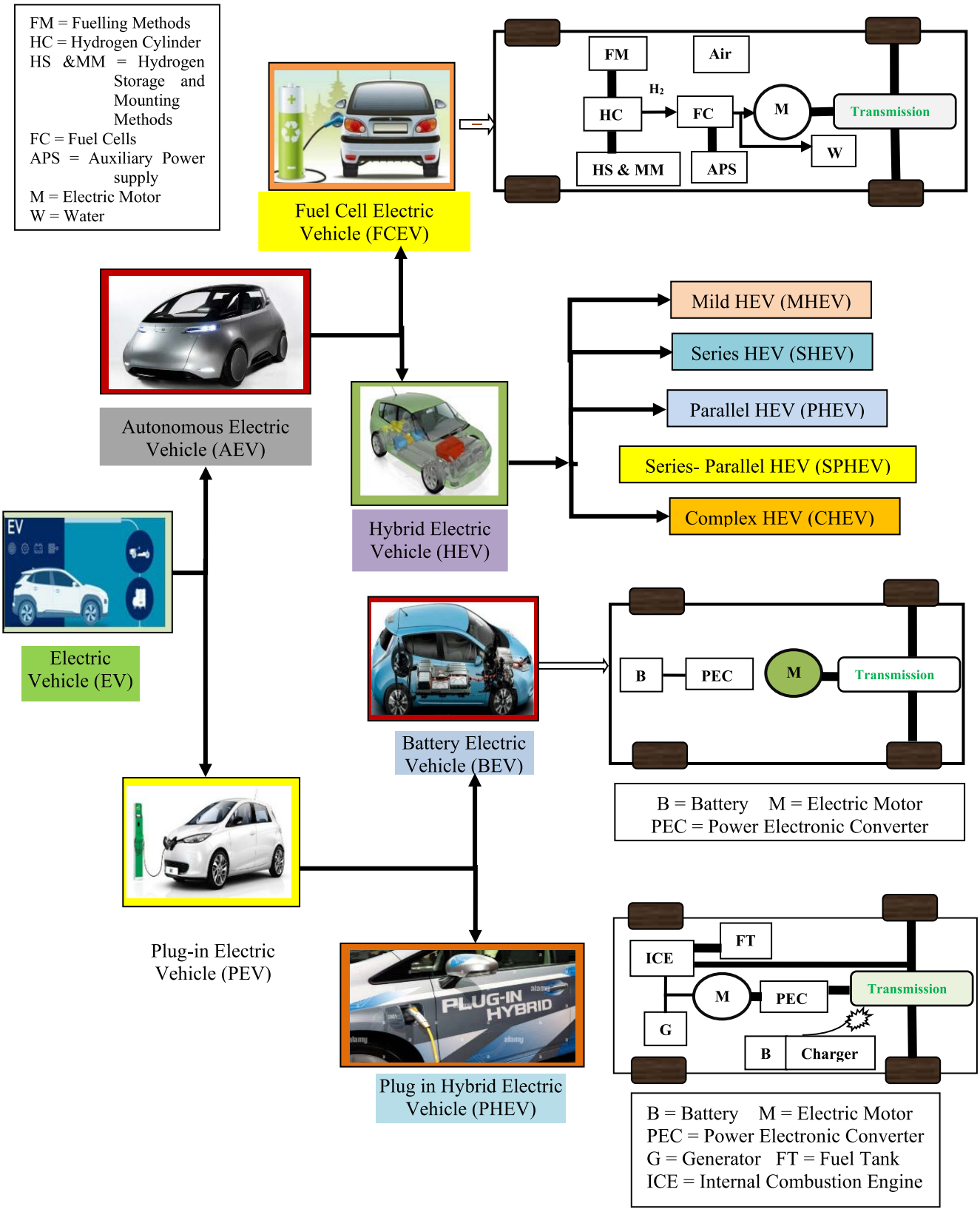

FIGURE 7. Various types of EV Classification.

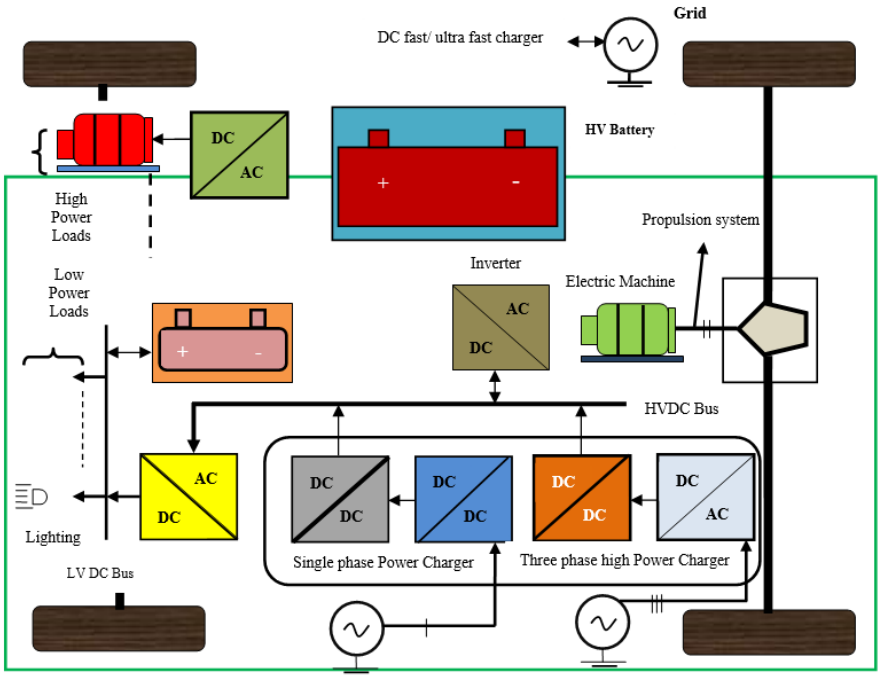

FIGURE 8. EV with Power Electronic converters.

TABLE 2. Switching operation of power electronic devices.

Parameter	Transistor	IGBT	MOSFET
Switching Rate	Medium	Fast	Very fast
price	Low	Low	High
Control method	Current	Voltage	Voltage
Drop in voltage	Low	Medium	High
Voltage Rating	Medium	Medium	Low
power organization	High	Low	Low

the rate of the charging station is directly proportional to the battery charging time. The comparison of various switching methods is described in Table 2.

To maintain less amount of charging time rapid chargers are developed. Commercially available electric vehicles can use charge stations with a greater maximum charge rate. This means that the battery is being charged at its maximum rate without any problems. As the temperature drops, the charging rate of the battery with a quick charger decreases [64], [66]. The charging speed of an EV battery is used to classify the chargers observed in Table 3.

TABLE 3. Types of EV chargers.

Parameter	Level-I	Level-II	DC Fast Charger
Output Voltage (V_0)	120V	240V	1000V
Source	On board converter	Public place or Workplace	Charging Stations
Charging Time (T_c)	8h	4h	30min
Driving Range	120km	130km	145km

H. EV SECURITY NECESSITIES

The electric vehicle must meet the safety criteria of the area regulations. Temperature, short circuit, fire impact, vibration, humidity, and water immersion are just a few of the conditions that the batteries must survive. Not only the above safety requirements but also collision detection, short circuit detection, and insulation should all be included in high-voltage transmission lines [67].

I. ENVIRONMENTAL IMPACT

Electric vehicles do not ruin the environment in general, but the components of the batteries are quarried or harvested from saline in the desert. This extraction has a low environmental impact on mining [68].

J. DRIVING RANGE

EVs have a lower driving range than comparable IC engine vehicles. Furthermore, the driving range is acknowledged as

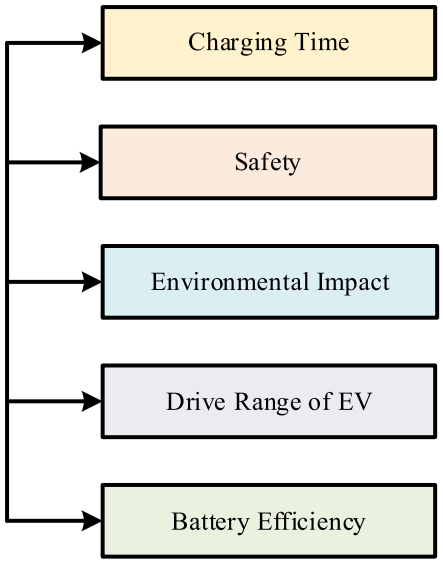

FIGURE 9. Classifications of Technical Issues in EV.

the most important factor. The range of an EV on a full charge or tank is seen as a significant disadvantage when compared to IC engine vehicles [69]. The above-mentioned technical barriers are represented as shown in Fig.9.

K. BATTERY PERFORMANCE

Electric vehicles are manufactured with electric motors, batteries, chargers and controllers by replacing energy tanks and gasoline engines of usual vehicles. At present, most manufacturers are offering eight years/120,600-mile warranty for their batteries [70], [71].

IV. ELECTROMAGNETIC INTERFERENCE (EMI)

In addition, the operational technical barriers of EVs are mitigation of EMI, EMC, and switching losses produced by the power electronic converters. The harmonic currents are responsible for these issues [72]. PWM-based controllers and DSP based DC-DC signal controllers are used to reduce the above-mentioned operational issues, which are represented as shown in Fig. 10(a)-(b). Two power switches (S_1^I and S_2^I) are available for managing the converter, C_1 and C_2 (two capacitors) are used to reduce ripple voltage, L is an interconnected inductor, and the DC/DC converter is used to convert between the DC source of the battery pack ($V_{dc\ Battery}$) and the DC link voltage ($V_{dc\ link}$) in a bidirectional manner.

The DC/DC converter acts as a boost type for charging the battery by appropriately managing S_1^I to regulate the voltage and switching off S_2^I to work as a freewheeling diode. The AC/DC converter is also utilized as a bidirectional converter for the DC link voltage and the AC voltage V_{ac} of the power grid, The H-bridge architecture as illustrated in Fig. 10 (a). The switches can be grouped in pairs to transition from DC to AC power. The PWM-driven S_2 and S_4 as well as the switched-off S_1 and S_3 change the positive portion of the resulting AC power, but the negative component can be regulated in the reverse direction, with PWM pulses driving S_1 and S_3 and switching off S_2 and S_4.

The converter operates as a full-bridge uncontrolled rectifier when all power switches are off, by converting power from one source to another [73]. The inductive and Capacitive filters i.e., L_f and C_f are single-stage EMI filters with damping branch circuits R_d and C_b, where R_d is the damping resistor and C_b is the dc-blocking capacitor, as shown in Fig. 10 (b). The battery impedance, the filter input impedance, the filter output impedance, and the converter input impedances are represented as Z_{Batt}, Z_{IF}, Z_{OF}, and Z_{IC}, respectively.

The frequency spectrum of the current disturbance is shown in Fig.11.The theoretical asymptotic envelope of amplitude spectrum is also shown in the same picture. The theoretical asymptotic envelope was determined by assuming rise time (t_R) = fall time (t_F) = 50 ns; it has a first cutoff frequency of $f1 = 1/(\pi t_R) = 636$ kHz. The present frequency spectrum includes considerable frequency content up to f2. Electromagnetic interference (EMI) is one of the most difficult problems to solve in the manufacturing of any electronic equipment. To comprehend and quantify the electromagnetic compatibility (EMC) of the instrument under test, the influence of these inevitable interferences on the instrument performance is carefully monitored. If the System EMI profile fails to satisfy accepted criteria, measures must be taken to mitigate the impact of these undesirable interferences so that the equipment may be utilized in an actual way [74], [78]. The electromagnetic interference (EMI) associated with a device is evaluated in order to assess its immunity and the quantity of interference.

EMI causes electrical equipment performance is degraded by introducing unnecessary currents and voltages in the circuitry. The behavior of EMI/EMC with respect to voltage and current is depicted in Fig.12.

V. TEMPERATURE EFFECT

Extreme temperature causes severe limitations to EV performance and its charging behaviour, the battery management system plays important role in the thermal sensitivity of the battery [79].

A. BATTERY MODEL

An artificial neural network (ANN) heating model, an ampere-hour (Ah) counter model, and an empirical voltage model make up the battery model. There are four sub modules: such as charging, discharging, high temperature, and low temperature are included in the voltage model. The input to the model is current, battery temperature, and State of Charge (SOC). The output voltage (V_{cell}) of the battery depends on the number of cells in series (N_S), the battery temperature (^{0}C) and SOC is given as

$$V(I, T_b, SOC) = N_S \cdot V_{Cell}(I, T_b, SOC) \quad (20)$$

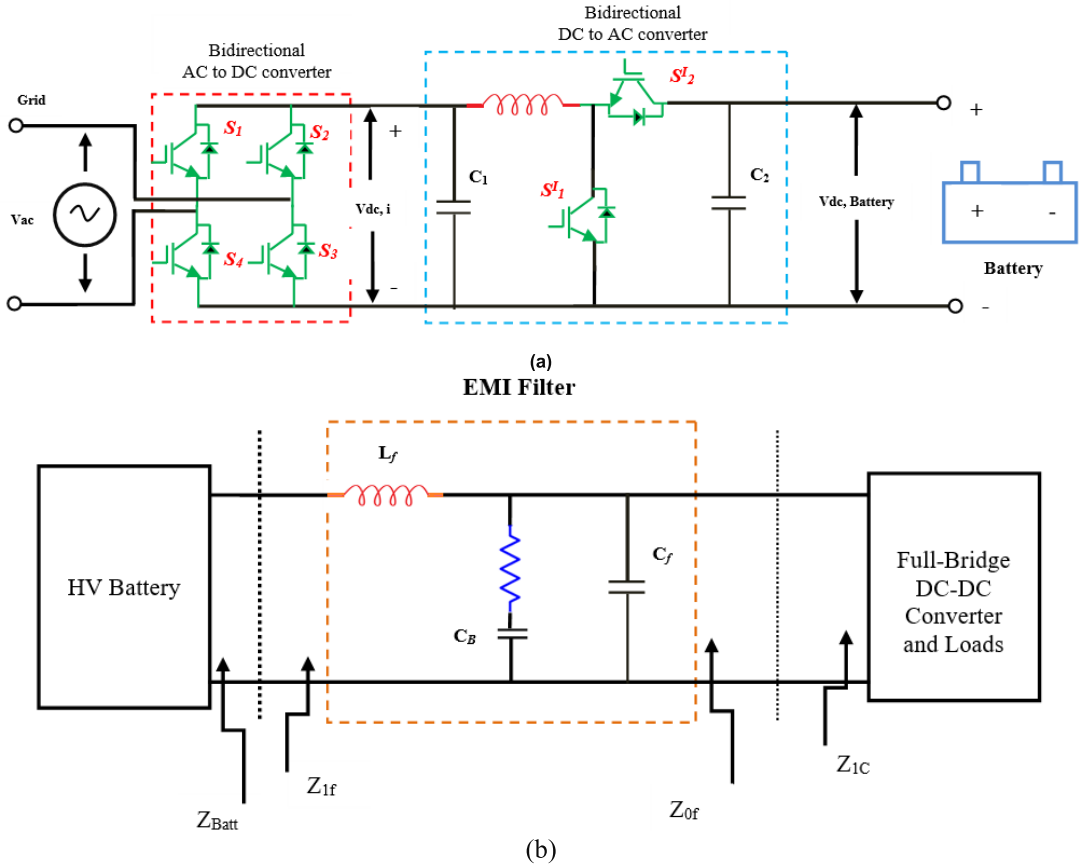

FIGURE 10. Mitigation of EV issues in PE converters using (a) PWM based controller (b) DSP controller impedance criterion.

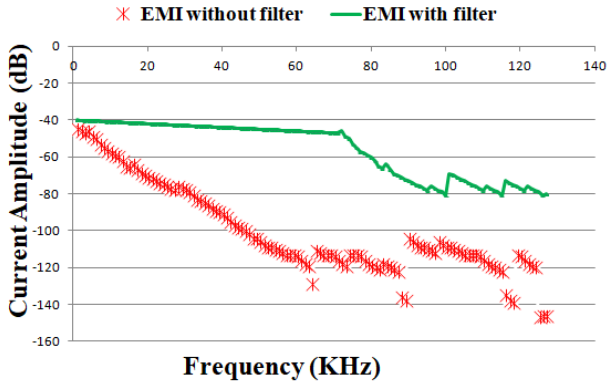

FIGURE 11. The frequency spectrum of Power electronic converter in terms of EMI with and without filter.

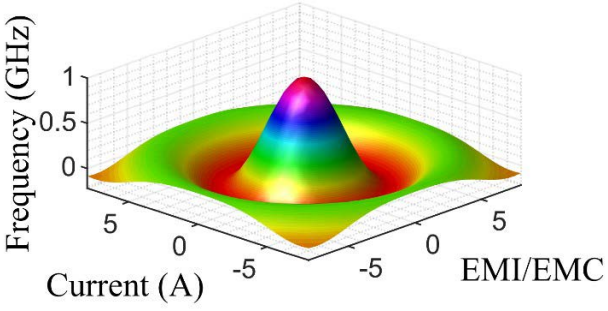

FIGURE 12. Characteristics of EMI with distorted current and at the corresponding frequency.

The neural network model evolves the Battery temperature during typical usage it takes the temperature of the battery and the state of charge as inputs and returns the batteries rate of heating (in^{0}C/ S). The internal heating of the battery is the product of heating rate (in^{0}C/ S) given by ANN ψ with the battery thermal mass (m_b) in (J/K) is

$$q_{int}(I, T_b, Z) = m_b \psi(I, T_b, Z) \tag{21}$$

The SOC of battery is given by

$$SOC_{t+1} = SOC_t - \frac{\Delta t \eta_c I}{C} \tag{22}$$

Δt is the length of time in step, η_C columbic charging and discharging efficiency, I denote current, while C is the battery pack's capacity in Ah. The Ah model does not consider battery age or deterioration.

B. THERMAL MODEL

The thermal model for the EV is a lumped capacitance model. The energy balance equations with respect to battery

TABLE 4. Determines the initial value for battery temperature (T_B) with Ambient temperature (T_A).

BTMS on standby	Initial value of T_B	Ambient temperature operation
Enabled	T_B standby, low	$T_A < T_B$ standby, low
Enabled	T_B standby, high	T_B standby, high $\leq T_a$
Disabled	T_A	None
Enabled	T_A	T_B standby, low $\leq T_a < T_B$, standby, high

temperature (T_b) is

$$T_{b,t+1} = T_{b,t} + \frac{\Delta t}{m_b}\left[\begin{array}{l} K_{a,b}(T_{a,t}-T_{b,t}) + K_{b,c}\left[T_{a,t}-T_{b,t}\right] + q_{int} \\ +(1-\eta_{inv+EM})\cdot P_{propulsion} + q_{BTMS} \end{array}\right] \quad (23)$$

Cabin temperature (T_C) is

$$T_{C,t+1} = T_{C,t} + \frac{\Delta t}{m_C}\left[\begin{array}{l} K_{a,C}(T_{a,t}-T_{C,t}) + K_{b,c}\left[T_{b,t}-T_{C,t}\right] \\ -K_{C,c}(T_{C,t}-T_{C,t}) + q_{HVAC} \end{array}\right] \quad (24)$$

where, m_b, m_C is the thermal of element (i), K is the heat transfer coefficient, q_{HVAC} is the actual heat flow due to HVAC operation.

q_{BTMS} is the actual heat flow due to BTMS operation. η_{inv+EM} are the combined efficiency of inverter and electric motor. Battery thermal management system plays an important for getting the desired output. The initial battery temperature is determined in Table 4. In EV, BTMS fails if the battery overheats (TB exceeds $+60^0$C). In practice, if BTMS fails, then the battery is overheated and lost thermal capacity results in degrading the performance of the battery. Therefore, BTMS maintains for battery at a temperature is less than $+20^0$C.

VI. BIDIRECTIONAL CHARGING STRATEGY

Bidirectional Electric Vehicle (BEV) charging systems achieve fast and dynamic response due to effective usage of power transfer [80], [82]. BEV is not only collected power from the grid to charge the EV battery, but also supplies power back to the grid. Depending upon the type of charging application BEV is classified as Vehicle to Grid (V2G), Vehicle to Home (V2H), and Vehicle to Load (V2L) charging system. Therefore, consumers mostly prefer BEV charging-based systems.

A. VEHICLE TO GRID (V2G)

In V2G charging scheme, the energy is absorbed from vehicle battery and simply delivered it to the utility grid. BEV-V2G charging system is depicted in Fig. 13(a).

B. VEHICLE TO HOME (V2H)

In V2H charging scheme, the energy from the battery is sent to the home or any other existing building. The conversion of energy is facilitated by DC to AC converter system which is internally linked with EV. Fig. 13(b), represents the V2H charging scheme in BEV.

C. VEHICLE TO LOAD (V2L)

V2L technology includes an onboard converter in the vehicle, which converts DC from the battery to AC. In V2L charging system the energy is transferred from EV battery to other vehicle or any other external electric loads. V2L charging scheme in BEV is represented as shown in Fig. 13 (c).

Bidirectional Charging System (BCS), completely monitors the active and reactive power flow between the grid and the EV battery and vice versa. BCS charger has two conversion stages one is AC to DC with the help of bridge rectifier and DC to DC using Buck-Boost Converter (BBC). The purpose of using controllers is to provide a proper power supply to the utility system. It is necessary to control the reactive power for regulating the grid voltage by incorporating the voltage-controlled strategy using AC to DC converter. The excess amount of reactive power is delivered to the DC link capacitor. In DC to DC converter the voltage is regulated and further involves in different modes of operation.

D. EXISTING BCS USING ARTIFICIAL NEURAL NETWORK

Bi-directional EV charging data is collected at regular intervals of time for ten days. These observations are considered in the form of the virtual system using MATLAB/Simulink process. ANN has two outputs, first signal controls the voltage levels through rectifier and DC link capacitor. Second signal control the charging current from the BBC. The important parameter observed using ANN strategy in BCS is to calculate the error between DC link voltage and the preset DC link voltage. The calculated error is sent to ANN training system for further computations which are in the form of phase shift angle. ANN-based BCS setup is depicted as shown in Fig. 14. The device built here has two inputs and two outputs (reference DC-link voltage and charging current). The training parameters are listed in table 5. DC link voltage and charging current are provided for the input as the ANN controller. The controller equations of BBC are mentioned in Eq. (25)-(32). The key operating equations for buck mode are from eq. (25)-(28), whereas boost mode is from Eq. (29)-(32).

EV battery voltage across the dc link is obtained as

$$V_{EV,B} = V_{DC,Link} - L_0 \frac{dI_{Charging}}{dt} \quad (25)$$

The charging current is obtained by integrating Eq. (25), and the complete voltage discharging cycle is given by

$$I_{Charging} = \frac{1}{L_0}\int_0^{T_0} (V_{DC,Link} - V_{EV,B}) \cdot dt \quad (26)$$

$$V_{BE,B} = -L_0 \cdot \frac{dI_{Charging}}{dt} \quad (27)$$

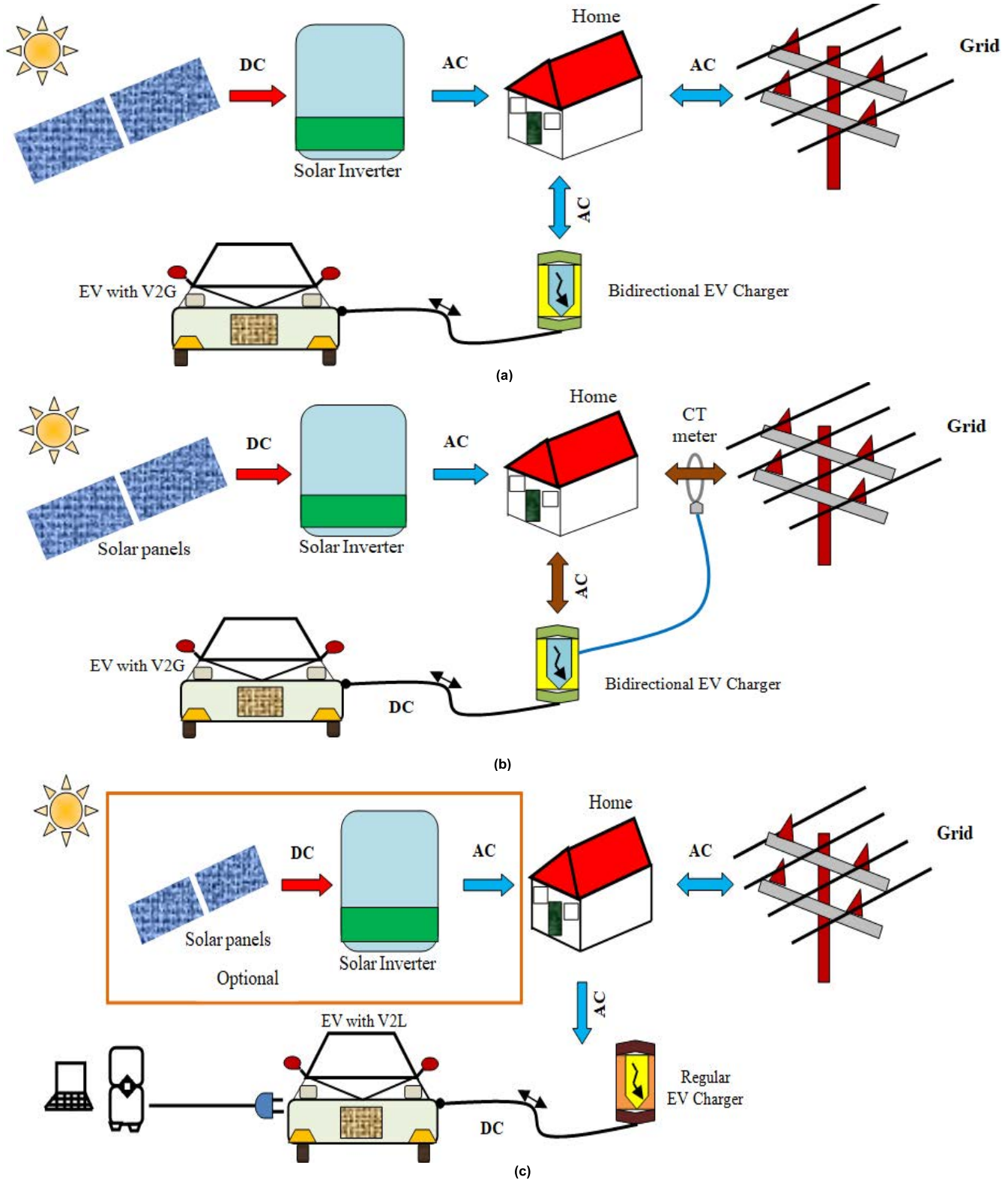

FIGURE 13. Bidirectional EV charging schemes (a) Vehicle to Grid (V2G), (b) Vehicle to Home (V2H), and (c) vehicle to Load (V2L) technology.

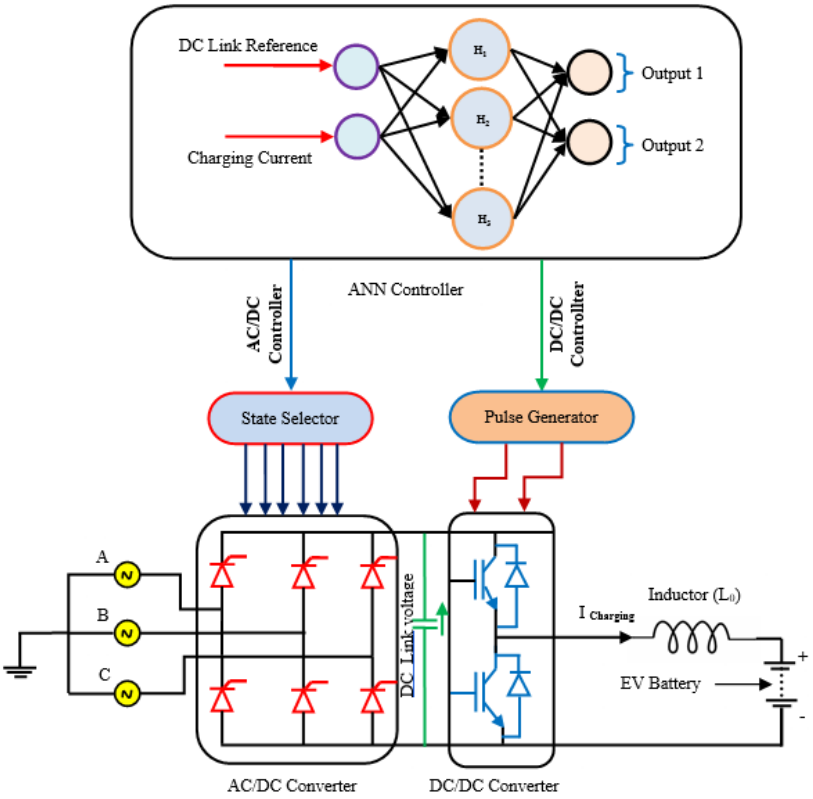

FIGURE 14. Bidirectional charging system using ANN Controller.

TABLE 5. Training parameters of ANN.

Parameter	Value
Testing Data	10%
Training Data	65%
Input Neuron	2
Evaluating Data	12%
Hidden layer	2
Iterations	50
Method	LM
Hidden Neuron	8

For a complete charging cycle, $I_{Charging}$ is given by

$$I_{Charging} = \int_{T_{ON}}^{T_{OFF}} \left(-\frac{V_{EV,B}}{L_0}\right) \cdot dt \tag{28}$$

$$V_{BE,B} = L_0 \cdot \frac{dI_{Charging}}{dt} \tag{29}$$

$$I_{Charging} = \frac{1}{L_0} \int_{0}^{T_0} (V_{EV,B}) \cdot dt \tag{30}$$

$V_{DC,Link}$ is input to the system, which is represented as

$$V_{EV,B} + V_{L0} = V_{DC,Link} \tag{31}$$

$$I_{Charging} = \frac{1}{L_0} \int_{T_{ON}}^{T_{OFF}} (V_{EV,B} + V_{DC,Link}) \cdot dt \tag{32}$$

From the above equations, a positive sign is representing charging and a negative sign for discharging the operation. ANN training process requires minimal error obtained between target result and the obtained result. The training process is based on classic Lavenberg-Marquardt (LM) based technique. The summative error is obtained as

$$E_j = Y_j - f(x_i, W^P_{K,N}) \tag{33}$$

$$E = \frac{1}{N} \sum_{j=1}^{N} E_j^2 \tag{34}$$

For any weight, the updated algorithm is given by

$$\gamma_{K+1} = \gamma_K - \beta_K^{-1} \cdot \delta_K \tag{35}$$

Here, $\gamma_K = W^P_{K,N} \cdot \beta_K \cdot \delta_K$ is treated as LM parameter.

E. BCS USING PROPOSED RECURRING NEURAL NETWORK TECHNIQUE

A recurrent neural network (RNN) is the modified form of ANN adapted for time series or sequential data. Purpose of

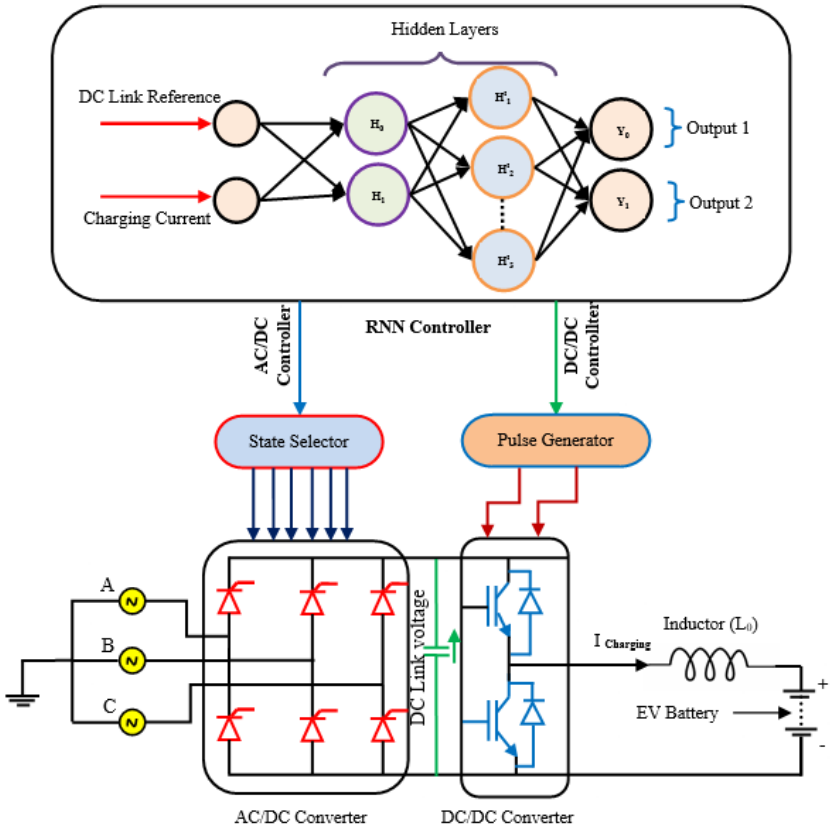

FIGURE 15. Bidirectional charging system using RNN Controller.

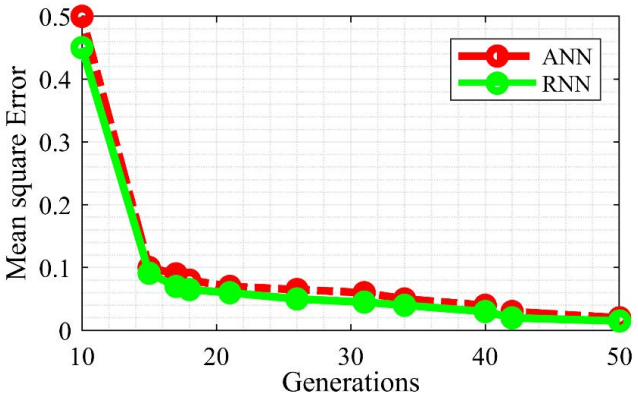

FIGURE 16. Mean square error response of ANN and proposed RNN technique.

TABLE 6. Training parameters of RNN.

Parameter	Value
Learning Rate	0.01
Training Data	70%
Input Neuron	2
Evaluating Data	12%
Hidden layers	2
Iterations/ RNN run time steps	50
Test Data	30%
Batch Size	20

using RNN in BCS of EV is to introducing the huge number of data with accurate propagation, i.e., multiple set of data can be acceptable in RNN. The training process is based on many to many data exchanging process depending on the type of input is provided for the training or computation process. The input to the RNN system is DC link voltage and charging current (same as ANN).

In ANN the system is limited to provide less quantity of error data, which results to increase the computation time and computation is non-uniform. RNN allows maximum number of error data and provide accurate computation levels to the system. During training process many hidden layers are participated in the error reduction process. The calculated error between actual battery current and reference battery current is minimum. Therefore, the battery system in EV is enhanced and improves the quality of the power conversion. The bidirectional charging system with RNN technique is depicted as shown in Fig. 15. The working parameters of RNN is observed in Table 6.

For all 50 generations, the error value of the ANN has been held constant from 0.1 to 0.06. Error levels for the proposed RNN approach have been lowered consistently to between 0.1 and 0.02. As a result of this, it has been established that the proposed RNN controller has a shorter amount of time to charge the system. The Mean Square Error (MSE) values of controllers are shown in Fig. 16, represents the performance of charging system with 50 generations. The error value is continuously dropping from 0.5 to 0.1 for less than 20 generations.

VII. CONCLUSION

This paper presents about real time general issues, operational issues, Battery charging and discharging phenomena, power electronic converter internal issues such as EMI, temperature effect and BCS conversion in EVs. The classification of various EVs such as FCEV, HEV, BEV, and PHEV are depicted in Fig.7. The switching operation of each IGBT, BJT, and MOSFET are listed in Table 2. EMI, EMC, and harmonic currents are

mainly responsible to minimizing the performance of EV. In circuitry, using the EMI filters and PWM based controllers are helpful to shave the peaky harmonics in the system. In this connection, it is benchmarked that the power electronic controllers mitigate the EMI/EMC and unnecessary currents in the circuitry also helpful to the other existing electronic devices. Advanced bidirectional charging system is incorporated to improve the performance of EV charging system. The power electronic components are using in the BCS, which lead to produce the error from the system, technically termed as Mean Square Error. The existing ANN controller acts as BCS charging system to reduce MSE value, but consumes much time due to uneven function of each generation. The results obtained in BCS using ANN controller is not optimum. Therefore, BCS is effectively improved using proposed RNN technique-based controller. The MSE error is eliminated in quick instant of time with a smaller number of generations. When compared to the ANN controller, the proposed RNN technique has a greater capacity to store information for each iteration.

REFERENCES

[1] R. Faria, P. Moura, J. Delgado, and A. T. de Almeida, "Managing the charging of electrical vehicles: Impacts on the electrical grid and on the environment," *IEEE Intell. Transp. Syst. Mag.*, vol. 6, no. 3, pp. 54–65, Dec. 2014, doi: 10.1109/MITS.2014.2323437.

[2] F. Salek, M. Babaie, M. M. Naserian, and M. H. Ahmadi, "Power enhancement of a turbo-charged industrial diesel engine by using of a waste heat recovery system based on inverted Brayton and organic Rankine cycles," *Fuel*, vol. 322, Aug. 2022, Art. no. 124036, doi: 10.1016/j.fuel.2022.124036.

[3] C. Wang, R. Liu, and A. Tang, "Energy management strategy of hybrid energy storage system for electric vehicles based on genetic algorithm optimization and temperature effect," *J. Energy Storage*, vol. 51, Jul. 2022, Art. no. 104314, doi: 10.1016/j.est.2022.104314.

[4] S. Rafique, M. S. H. Nizami, U. B. Irshad, M. J. Hossain, and S. C. Mukhopadhyay, "EV scheduling framework for peak demand management in LV residential networks," *IEEE Syst. J.*, vol. 16, no. 1, pp. 1520–1528, Mar. 2022, doi: 10.1109/JSYST.2021.3068004.

[5] R. N. E. Idrissi, M. Ouassaid, and M. Maaroufi, "A constrained programming-based algorithm for optimal scheduling of aggregated EVs power demand in smart buildings," *IEEE Access*, vol. 10, pp. 28434–28444, 2022, doi: 10.1109/ACCESS.2022.3154781.

[6] M. Murugan and S. Marisamynathan, "Analysis of barriers to adopt electric vehicles in India using fuzzy DEMATEL and relative importance index approaches," *Case Stud. Transp. Policy*, vol. 10, no. 2, pp. 795–810, Jun. 2022, doi: 10.1016/j.cstp.2022.02.007.

[7] E. Yao, T. Liu, T. Lu, and Y. Yang, "Optimization of electric vehicle scheduling with multiple vehicle types in public transport," *Sustain. Cities Soc.*, vol. 52, Jan. 2020, Art. no. 101862, doi: 10.1016/j.scs.2019.101862.

[8] D. Cittanti, E. Vico, and I. R. Bojoi, "New FOM-based performance evaluation of 600/650 V SiC and GaN semiconductors for next-generation EV drives," *IEEE Access*, vol. 10, pp. 51693–51707, 2022, doi: 10.1109/ACCESS.2022.3174777.

[9] S. Sharma, A. K. Panwar, and M. M. Tripathi, "Storage technologies for electric vehicles," *J. Traffic Transp. Eng. (English Ed.)*, vol. 7, no. 3, pp. 340–361, Jun. 2020, doi: 10.1016/j.jtte.2020.04.004.

[10] K. Zhou, H. Fang, and Y. Liu, "Driving–charging integrated controller for electric vehicles," *IEEE Access*, vol. 10, pp. 66545–66563, 2022, doi: 10.1109/ACCESS.2022.3185261.

[11] W. Li, J. Fang, H. Li, and J. Tang, "Position sensorless control without phase shifter for high-speed BLDC motors with low inductance and nonideal back EMF," *IEEE Trans. Power Electron.*, vol. 31, no. 2, pp. 1354–1366, Feb. 2016, doi: 10.1109/TPEL.2015.2413593.

[12] F. U. Haq, P. Bhui, and K. Chakravarthi, "Real time congestion management using plug in electric vehicles (PEV's): A game theoretic approach," *IEEE Access*, vol. 10, pp. 42029–42043, 2022, doi: 10.1109/ACCESS.2022.3167847.

[13] A. T. Al-awami and S. Member, "An autonomous charge controller for electric vehicles using online sensitivity estimation," *IEEE Trans. Ind. Appl.*, vol. 56, no. 1, pp. 22–33, Jan./Feb. 2020.

[14] H. Zhao, Y. Shen, W. Ying, S. S. Ghosh, M. R. Ahmed, and T. Long, "A single- and three-phase grid compatible converter for electric vehicle on-board chargers," *IEEE Trans. Power Electron.*, vol. 35, no. 7, pp. 7545–7562, Jul. 2020, doi: 10.1109/TPEL.2019.2956653.

[15] S. Park and C. Ahn, "Computationally efficient stochastic model predictive controller for battery thermal management of electric vehicle," *IEEE Trans. Veh. Technol.*, vol. 69, no. 8, pp. 8407–8419, Aug. 2020.

[16] M. Khalid, F. Ahmad, B. K. Panigrahi, and L. Al-Fagih, "A comprehensive review on advanced charging topologies and methodologies for electric vehicle battery," *J. Energy Storage*, vol. 53, Sep. 2022, Art. no. 105084, doi: 10.1016/j.est.2022.105084.

[17] V. Indragandhi, R. Selvamathi, D. Gunapriya, B. Balagurunathan, G. Suresh, and A. Chitra, "An efficient regenerative braking system based on battery- ultracapacitor for electric vehicles," in *Proc. Innov. Power Adv. Comput. Technol. (i-PACT)*, Nov. 2021, vol. 2021, vol. 66, no. 5, pp. 3724–3738, doi: 10.1109/i-PACT52855.2021.9696557.

[18] Y. Fu et al., "Design methodology of a three-phase four-wire EV charger operated at the autonomous mode," *IEEE Trans. Transport Electrific.*, vol. 5, no. 4, pp. 1169–1181, Dec. 2019, doi: 10.1109/TTE.2019.2957635.

[19] M. S. Wasim, S. Habib, M. Amjad, A. R. Bhatti, E. M. Ahmed, and M. A. Qureshi, "Battery-ultracapacitor hybrid energy storage system to increase battery life under pulse loads," *IEEE Access*, vol. 10, pp. 62173–62182, 2022, doi: 10.1109/ACCESS.2022.3182468.

[20] A. Stirban, I. Boldea, and G.-D. Andreescu, "Motion-sensorless control of BLDC-PM motor with offline FEM-information-assisted position and speed observer," *IEEE Trans. Ind. Appl.*, vol. 48, no. 6, pp. 1950–1958, Nov. 2012, doi: 10.1109/TIA.2012.2226194.

[21] D. Mishra, B. Singh, and B. Ketan Panigrahi, "Sigma-modified power control and parametric adaptation in a grid-integrated PV for EV charging architecture," *IEEE Trans. Energy Convers.*, vol. 37, no. 3, pp. 1965–1976, Sep. 2022, doi: 10.1109/TEC.2022.3145884.

[22] E. Dokur, N. Erdogan, and S. Kucuksari, "EV fleet charging load forecasting based on multiple decomposition with CEEMDAN and swarm decomposition," *IEEE Access*, vol. 10, pp. 62330–62340, 2022, doi: 10.1109/ACCESS.2022.3182499.

[23] M. Baszynski and S. Pirog, "A novel speed measurement method for a high-speed BLDC motor based on the signals from the rotor position sensor," *IEEE Trans. Ind. Informat.*, vol. 10, no. 1, pp. 84–91, Feb. 2014, doi: 10.1109/TII.2013.2243740.

[24] G. Ala, M. C. D. Piazza, G. Tine, F. Viola, and G. Vitale, "Evaluation of radiated EMI in 42-V vehicle electrical systems by FDTD simulation," *IEEE Trans. Veh. Technol.*, vol. 56, no. 4, pp. 1477–1484, Jul. 2007, doi: 10.1109/TVT.2007.896964.

[25] X. Huang, H. Toshiyuki, and H. Hori Yoichi, "Energy management strategy based on frequency-varying filter for the battery supercapacitor hybrid system of electric vehicles," *World Electr. Vehicle J.*, vol. 6, no. 3, pp. 623–628, Sep. 2013, doi: 10.3390/wevj6030623.

[26] A. Battiston, E.-H. Miliani, S. Pierfederici, and F. Meibody-Tabar, "Efficiency improvement of a quasi-Z-source inverter-fed permanent-magnet synchronous machine-based electric vehicle," *IEEE Trans. Transport. Electrific.*, vol. 2, no. 1, pp. 14–23, Mar. 2016, doi: 10.1109/TTE.2016.2519349.

[27] Z. Zhang and K.-T. Chau, "Pulse-width-modulation-based electromagnetic interference mitigation of bidirectional grid-connected converters for electric vehicles," *IEEE Trans. Smart Grid*, vol. 8, no. 6, pp. 2803–2812, Nov. 2017, doi: 10.1109/TSG.2016.2541163.

[28] D. Hamza, M. Pahlevaninezhad, and P. K. Jain, "Implementation of a novel digital active EMI technique in a DSP-based DC–DC digital controller used in electric vehicle (EV)," *IEEE Trans. Power Electron.*, vol. 28, no. 7, pp. 3126–3137, Jul. 2013, doi: 10.1109/TPEL.2012.2223764.

[29] J. Lindgren and P. D. Lund, "Effect of extreme temperatures on battery charging and performance of electric vehicles," *J. Power Sources*, vol. 328, pp. 37–45, Oct. 2016, doi: 10.1016/j.jpowsour.2016.07.038.

[30] R. Alvarez and M. Weilenmann, "Effect of low ambient temperature on fuel consumption and pollutant and CO_2 emissions of hybrid electric vehicles in real-world conditions," *Fuel*, vol. 97, pp. 119–124, Jul. 2012, doi: 10.1016/j.fuel.2012.01.022.

[31] D. Han, C. T. Morris, W. Lee, and B. Sarlioglu, "A case study on common mode electromagnetic interference characteristics of GaN HEMT and Si MOSFET power converters for EV/HEVs," *IEEE Trans. Transp. Electrific.*, vol. 3, no. 1, pp. 168–179, Mar. 2017, doi: 10.1109/TTE.2016.2622005.

[32] P. Sun, J.-S. Lai, C. Liu, and W. Yu, "A 55-kW three-phase inverter based on hybrid-switch soft-switching modules for high-temperature hybrid electric vehicle drive application," *IEEE Trans. Ind. Appl.*, vol. 48, no. 3, pp. 962–969, May/Jun. 2012, doi: 10.1109/TIA.2012.2191169.

[33] S. H. Yu, D. J. Park, and K. C. Kim, "Heat source analysis of an induction heater for an electric vehicle," *IEEE Trans. Magn.*, vol. 53, no. 6, pp. 53–56, Jun. 2017, doi: 10.1109/TMAG.2017.2662946.

[34] Z. Wang, Y. Zhang, S. You, H. Xiao, and M. Cheng, "An integrated power conversion system for electric traction and V2G operation in electric vehicles with a small film capacitor," *IEEE Trans. Power Electron.*, vol. 35, no. 5, pp. 5066–5077, May 2020, doi: 10.1109/TPEL.2019.2944276.

[35] Y. Zhang, Y. Gao, L. Zhou, and M. Sumner, "A switched-capacitor bidirectional DC–DC converter with wide voltage gain range for electric vehicles with hybrid energy sources," *IEEE Trans. Power Electron.*, vol. 33, no. 11, pp. 9459–9469, Nov. 2018, doi: 10.1109/TPEL.2017.2788436.

[36] Y. Yao, S. Gao, Y. Wang, X. Liu, X. Zhang, and D. Xu, "Design and optimization of an electric vehicle wireless charging system using interleaved boost converter and flat solenoid coupler," *IEEE Trans. Power Electron.*, vol. 36, no. 4, pp. 3894–3908, Apr. 2021, doi: 10.1109/TPEL.2020.3019441.

[37] A. Sheir, M. Z. Youssef, and M. Orabi, "A novel bidirectional T-type multilevel inverter for electric vehicle applications," *IEEE Trans. Power Electron.*, vol. 34, no. 7, pp. 6648–6658, Jul. 2019, doi: 10.1109/TPEL.2018.2871624.

[38] L. Dorn-Gomba, P. Magne, B. Danen, and A. Emadi, "On the concept of the multi-source inverter for hybrid electric vehicle powertrains," *IEEE Trans. Power Electron.*, vol. 33, no. 9, pp. 7376–7386, Sep. 2018, doi: 10.1109/TPEL.2017.2765247.

[39] R. Shi, S. Semsar, and P. W. Lehn, "Constant current fast charging of electric vehicles via a DC grid using a dual-inverter drive," *IEEE Trans. Ind. Electron.*, vol. 64, no. 9, pp. 6940–6949, Sep. 2017, doi: 10.1109/TIE.2017.2686362.

[40] Y. Han, H. Lu, Y. Li, and J. Chai, "Analysis and suppression of shaft voltage in SiC-based inverter for electric vehicle applications," *IEEE Trans. Power Electron.*, vol. 34, no. 7, pp. 6276–6285, Jul. 2019, doi: 10.1109/TPEL.2018.2873079.

[41] Z. Du, B. Ozpineci, L. M. Tolbert, and J. N. Chiasson, "DC-AC cascaded H-bridge multilevel boost inverter with no inductors for electric/hybrid electric vehicle applications," *IEEE Trans. Ind. Appl.*, vol. 45, no. 3, pp. 963–970, May 2009, doi: 10.1109/TIA.2009.2018978.

[42] M. Bayati, M. Abedi, M. Farahmandrad, G. B. Gharehpetian, and K. Tehrani, "Important technical considerations in design of battery chargers of electric vehicles," *Energies*, vol. 14, no. 18, p. 5878, Sep. 2021, doi: 10.3390/en14185878.

[43] M. Brenna, G. C. Lazaroiu, M. Roscia, and S. Saadatmandi, "Dynamic model for the EV's charging infrastructure planning through finite element method," *IEEE Access*, vol. 8, pp. 102399–102408, 2020, doi: 10.1109/ACCESS.2020.2998783.

[44] H. Chen, S. Lou, and C. Lv, "Hybrid physics-data-driven online modelling: Framework, methodology and application to electric vehicles," *Mech. Syst. Signal Process.*, vol. 185, Feb. 2023, Art. no. 109791, doi: 10.1016/j.ymssp.2022.109791.

[45] L. Maybury, P. Corcoran, and L. Cipcigan, "Mathematical modelling of electric vehicle adoption: A systematic literature review," *Transp. Res. D, Transp. Environ.*, vol. 107, Jun. 2022, Art. no. 103278, doi: 10.1016/j.trd.2022.103278.

[46] M. S. Miah, "Optimized energy management schemes for electric vehicle applications: A bibliometric analysis towards future trends," *Sustainability*, vol. 13, no. 22, p. 12800, 2021, doi: 10.3390/su132212800.

[47] R. S. Gupta, A. Tyagi, and S. Anand, "Optimal allocation of electric vehicles charging infrastructure, policies and future trends," *J. Energy Storage*, vol. 43, Nov. 2021, Art. no. 103291, doi: 10.1016/j.est.2021.103291.

[48] M. Bayati, M. Abedi, M. Farahmandrad, G. B. Gharehpetian, and K. Tehrani, "Important technical considerations in design of battery chargers of electric vehicles," *Energies*, vol. 14, no. 18, p. 5878, 2021, doi: 10.3390/en14185878.

[49] T. Palit, A. B. M. M. Bari, and C. L. Karmaker, "An integrated principal component analysis and interpretive structural modeling approach for electric vehicle adoption decisions in sustainable transportation systems," *Decis. Anal. J.*, vol. 4, Sep. 2022, Art. no. 100119, doi: 10.1016/j.dajour.2022.100119.

[50] G. Bridge and E. Faigen, "Towards the lithium-ion battery production network: Thinking beyond mineral supply chains," *Energy Res. Social Sci.*, vol. 89, Jul. 2022, Art. no. 102659, doi: 10.1016/j.erss.2022.102659.

[51] S. Comello, G. Glenk, and S. Reichelstein, "Transitioning to clean energy transportation services: Life-cycle cost analysis for vehicle fleets," *Appl. Energy*, vol. 285, Mar. 2021, Art. no. 116408, doi: 10.1016/j.apenergy.2020.116408.

[52] K. Jyotheeswara Reddy and S. Natarajan, "Energy sources and multi-input DC–DC converters used in hybrid electric vehicle applications—A review," *Int. J. Hydrogen Energy*, vol. 43, no. 36, pp. 17387–17408, Sep. 2018, doi: 10.1016/j.ijhydene.2018.07.076.

[53] A. Khaligh and Z. Li, "Battery, ultracapacitor, fuel cell, and hybrid energy storage systems for electric, hybrid electric, fuel cell, and plug-in hybrid electric vehicles: State of the art," *IEEE Trans. Veh. Technol.*, vol. 59, no. 6, pp. 2806–2814, Jul. 2010, doi: 10.1109/TVT.2010.2047877.

[54] A. F. Burke, "Batteries and ultracapacitors for electric, hybrid, and fuel cell vehicles," *Proc. IEEE*, vol. 95, no. 4, pp. 806–820, Apr. 2007, doi: 10.1109/JPROC.2007.892490.

[55] W. Kim, P.-Y. Lee, J. Kim, and K.-S. Kim, "A robust state of charge estimation approach based on nonlinear battery cell model for lithium-ion batteries in electric vehicles," *IEEE Trans. Veh. Technol.*, vol. 70, no. 6, pp. 5638–5647, Jun. 2021, doi: 10.1109/TVT.2021.3079934.

[56] A. Rezaei, J. B. Burl, M. Rezaei, and B. Zhou, "Catch energy saving opportunity in charge-depletion mode, a real-time controller for plug-in hybrid electric vehicles," *IEEE Trans. Veh. Technol.*, vol. 67, no. 11, pp. 11234–11237, Nov. 2018, doi: 10.1109/TVT.2018.2866569.

[57] P. K. Maroti, S. Padmanaban, M. S. Bhaskar, V. K. Ramachandaramurthy, and F. Blaabjerg, "The state-of-the-art of power electronics converters configurations in electric vehicle technologies," *Power Electron. Devices Compon.*, vol. 1, Mar. 2022, Art. no. 100001, doi: 10.1016/j.pedc.2021.100001.

[58] M. Inci, M. M. Savrun, and Ö. Çelik, "Integrating electric vehicles as virtual power plants: A comprehensive review on vehicle-to-grid (V2G) concepts, interface topologies, marketing and future prospects," *J. Energy Storage*, vol. 55, Nov. 2022, Art. no. 105579, doi: 10.1016/j.est.2022.105579.

[59] A. Emadi, A. Khaligh, C. H. Rivetta, and G. A. Williamson, "Constant power loads and negative impedance instability in automotive systems: Definition, modeling, stability, and control of power electronic converters and motor drives," *IEEE Trans. Veh. Technol.*, vol. 55, no. 4, pp. 1112–1125, Jul. 2006, doi: 10.1109/TVT.2006.877483.

[60] Y. Xie, Z. Liu, K. Li, J. Liu, Y. Zhang, D. Dan, C. Wu, P. Wang, and X. Wang, "An improved intelligent model predictive controller for cooling system of electric vehicle," *Appl. Thermal Eng.*, vol. 182, Jan. 2021, Art. no. 116084, doi: 10.1016/j.applthermaleng.2020.116084.

[61] J. Fleischer, E. Gerlitz, S. Rieß, S. Coutandin, and J. Hofmann, "Concepts and requirements for flexible disassembly systems for drive train components of electric vehicles," *Proc. CIRP*, vol. 98, pp. 577–582, Jan. 2021, doi: 10.1016/j.procir.2021.01.154.

[62] I. Husain, B. Ozpineci, M. S. Islam, E. Gurpinar, G.-J. Su, W. Yu, S. Chowdhury, L. Xue, D. Rahman, and R. Sahu, "Electric drive technology trends, challenges, and opportunities for future electric vehicles," *Proc. IEEE*, vol. 109, no. 6, pp. 1039–1059, Jun. 2021, doi: 10.1109/JPROC.2020.3046112.

[63] R. Chen, X. Qian, L. Miao, and S. V. Ukkusuri, "Optimal charging facility location and capacity for electric vehicles considering route choice and charging time equilibrium," *Comput. Oper. Res.*, vol. 113, Jan. 2020, Art. no. 104776, doi: 10.1016/j.cor.2019.104776.

[64] F. Blaabjerg, H. Wang, I. Vernica, B. Liu, and P. Davari, "Reliability of power electronic systems for EV/HEV applications," *Proc. IEEE*, vol. 109, no. 6, pp. 1060–1076, Jun. 2021, doi: 10.1109/JPROC.2020.3031041.

[65] A. G. Olabi et al., "Battery electric vehicles: Progress, power electronic converters, strength (S), weakness (W), opportunity (O), and threats (T)," *Int. J. Thermofluids*, vol. 16, Nov. 2022, Art. no. 100212.

[66] G. Fridgen, M. Thimmel, M. Weibelzahl, and L. Wolf, "Smarter charging: Power allocation accounting for travel time of electric vehicle drivers," *Transp. Res. D, Transp. Environ.*, vol. 97, Aug. 2021, Art. no. 102916, doi: 10.1016/j.trd.2021.102916.

[67] Y. Dahmane, R. Chenouard, M. Ghanes, and M. Alvarado-Ruiz, "Optimized time step for electric vehicle charging optimization considering cost and temperature," *Sustain. Energy, Grids Netw.*, vol. 26, Jun. 2021, Art. no. 100468, doi: 10.1016/j.segan.2021.100468.

[68] A. Picatoste, D. Justel, J. Manuel, and F. Mendoza, "Circularity and life cycle environmental impact assessment of batteries for electric vehicles: Industrial challenges, best practices and research guidelines," *Renew. Sustain. Energy Rev.*, vol. 169, Nov. 2022, Art. no. 112941.

[69] M. Feizi and R. Beiranvand, "An improved phase-shifted full-bridge converter with extended ZVS operation range for EV battery charger applications," in *Proc. 11th Power Electron., Drive Syst., Technol. Conf. (PEDSTC)*, Feb. 2020, doi: 10.1109/PEDSTC49159.2020.9088444.

[70] C. Shilaja, S. R. Kiran, M. Murali, S. M. Khaja Moinuddin, K. Navani, S. Yousuf, and M. Harshith, "Design and analysis of global optimization methods for proton exchange membrane fuel cell powered electric vehicle system with single switch DC–DC converter," *Mater. Today: Proc.*, vol. 52, pp. 2057–2064, Jan. 2022, doi: 10.1016/j.matpr.2021.12.204.

[71] D. Strickland, L. Chittock, D. A. Stone, M. P. Foster, and B. Price, "Estimation of transportation battery second life for use in electricity grid systems," *IEEE Trans. Sustain. Energy*, vol. 5, no. 3, pp. 795–803, Jul. 2014, doi: 10.1109/TSTE.2014.2303572.

[72] L. Zhai, G. Hu, M. Lv, T. Zhang, and R. Hou, "Comparison of two design methods of EMI filter for high voltage power supply in DC–DC converter of electric vehicle," *IEEE Access*, vol. 8, pp. 66564–66577, 2020, doi: 10.1109/ACCESS.2020.2985528.

[73] X. Gong, I. Josifović, and J. A. Ferreira, "Modeling and reduction of conducted EMI of inverters with SiC JFETs on insulated metal substrate," *IEEE Trans. Power Electron.*, vol. 28, no. 7, pp. 3138–3146, Jul. 2013, doi: 10.1109/TPEL.2012.2221747.

[74] S. W. Pasko, M. K. Kazimierczuk, and B. Grzesik, "Self-capacitance of coupled Toroidal inductors for EMI filters," *IEEE Trans. Electromagn. Compat.*, vol. 57, no. 2, pp. 216–223, Apr. 2015, doi: 10.1109/TEMC.2014.2378535.

[75] H. Chen, T. Wang, S. Ye, and T. Zhou, "Modeling and suppression of electromagnetic interference noise on motor resolver of electric vehicle," *IEEE Trans. Electromagn. Compat.*, vol. 63, no. 3, pp. 720–729, Jun. 2021, doi: 10.1109/TEMC.2020.3023088.

[76] J. Hu, X. Xu, D. Cao, and G. Liu, "Analysis and optimization of electromagnetic compatibility for electric vehicles," *IEEE Electromagn. Compat. Mag.*, vol. 8, no. 4, pp. 50–55, 2019, doi: 10.1109/MEMC.2019.8985599.

[77] I. Echeverria, F. Arteche, M. Iglesias, A. Pradas, J. Piedrafita, and F. J. Arcega, "Common mode noise propagation and effects in a four-wheel drive electric vehicle," *IEEE Trans. Electromagn. Compat.*, vol. 60, no. 1, pp. 132–139, Feb. 2018, doi: 10.1109/TEMC.2017.2701885.

[78] X. Jia and Z. University, "Influence of system layout on CM EMI noise of SiC electric vehicle powertrains," *CPSS Trans. Power Electron. Appl.*, vol. 6, no. 4, pp. 298–309, Dec. 2021, doi: 10.24295/cpsstpea.2021.00028.

[79] V. Kulkarni, G. Ghaisas, and S. Krishnan, "Performance analysis of an integrated battery electric vehicle thermal management," *J. Energy Storage*, vol. 55, Nov. 2022, Art. no. 105334, doi: 10.1016/j.est.2022.105334.

[80] D. Mishra, B. Singh, and B. Ketan Panigrahi, "Adaptive current control for a bidirectional interleaved EV charger with disturbance rejection," *IEEE Trans. Ind. Appl.*, vol. 57, no. 4, pp. 4080–4090, Aug. 2021, doi: 10.1109/TIA.2021.3074612.

[81] K. Schwenk, S. Meisenbacher, B. Briegel, T. Harr, V. Hagenmeyer, and R. Mikut, "Integrating battery aging in the optimization for bidirectional charging of electric vehicles," *IEEE Trans. Smart Grid*, vol. 12, no. 6, pp. 5135–5145, Nov. 2021, doi: 10.1109/TSG.2021.3099206.

[82] R. K. Phanden, R. Gupta, S. R. Gorrepati, P. Patel, and L. Sharma, "ANN based robust bidirectional charger for electric vehicles," *Mater. Today: Proc.*, vol. 38, pp. 80–84, Jan. 2021, doi: 10.1016/j.matpr.2020.05.828.

SAIRAJ ARANDHAKAR (Member, IEEE) was born in India, in 1990. He received the B.Tech. degree in electrical and electronics engineering from the Vaagdevi College of Engineering, Warangal, Telangana, India, in 2013, and the M.Tech. degree from the CVR College of Engineering, Hyderabad, Telangana, in 2020. He is currently working as a Research Scholar with the Department of Electrical Engineering, National Institute of Technology Andhra Pradesh, India. His research interests include BLDC motors, electric vehicles, and machine learning.

NAKKA JAYARAM received the B.Tech. degree in electrical and electronics engineering from Jawaharlal Nehru Technological University, Hyderabad, India, in 2007, the M.Tech. degree from the Vellore Institute of Technology, Vellore, India, in 2009, and the Ph.D. degree in electrical engineering from the Indian Institute of Technology, Roorkee, India, in 2014. He is currently with the Department of Electrical Engineering, National Institute of Technology Andhra Pradesh, India. He has published many international and national journals and conferences. He is a reviewer of many international journals. His research interests include multilevel inverters, high-power converters, and renewable energy systems.

YANNAM RAVI SHANKAR was born in July 1986. He received the B.Tech. degree in electrical and electronics engineering from the Prakasam Engineering College, JNTU Hyderabad, Andhra Pradesh, India, in 2008, and the M.Tech. degree in power and industrial drives from JNTU Kakinada, India, in 2011. He worked two years as an Assistant Professor with the SSN Engineering College, Ongole, Andhra Pradesh. He is currently working as an Assistant Professor with Dire Dawa University, Dire Dawa, Ethiopia. His research interests include power electronics, power systems, advanced control systems, and electrical machines.

GAURAV (Student Member, IEEE) received the B.Tech. degree in electrical engineering from Dr. A. P. J. Abdul Kalam Technical University (AKTU), Greater Noida, India, in 2018, and the M.Tech. degree in electrical power and energy systems from the National Institute of Technology, Srinagar (JK), India, in 2020. He is currently pursuing the Ph.D. degree with the National Institute of Technology Andhra Pradesh, India. His research interests include high-gain dc–dc converters, multilevel inverters, non-isolated bidirectional converters, power electronics, and ac motor drives and control.

PULAVARTHI SATYA VENKATA KISHORE (Student Member, IEEE) received the B.E. degree in electrical and electronics engineering from Andhra University, India, in 2009, the M.Tech. degree in power electronics from the National Institute of Technology, Calicut, India, in 2011, and the Ph.D. degree from the National Institute of Technology Andhra Pradesh, India. He worked as an Assistant Professor with the Vignan's Institute of Information Technology, India, for five years and in Dire Dawa University, Ethiopia, for three years. He is currently working as an Assistant Professor with the Sri Vasavi Engineering College, Tadepalligudem, India. His research interests include multilevel inverters, high-power factor converters, grid integration of renewable energy systems, and power electronics.

SUKANTA HALDER (Member, IEEE) received the B.Tech. degree in electrical engineering from the Jalpaiguri Government Engineering College, and the M.Tech. degree with the specialization in electric drives and power electronics and the Ph.D. degree in electrical engineering from the Indian Institute of Technology (IIT) Roorkee, India, in 2017. He is currently an Assistant Professor with the Department of Electrical Engineering, Sardar Vallabhbhai National Institute of Technology (SVNIT), Surat, India. After Ph.D., in 2017, he joined with the Rolls-Royce@NTU Corporate Laboratory, Nanyang Technological University, Singapore, as a Postdoctoral Fellow. He worked with Rolls-Royce Electrical, Singapore, Nanyang Technological University, which is holding QS world ranking 4th in electrical engineering. He joined the Charge Laboratory, University of Windsor, Windsor, ON, Canada, which is the one of the biggest EV Laboratory in North America under Tier 1 Canada Research Chair Professor in Electrified Vehicles. He was involved for developing WBG-based inverter and intelligent control for EV in collaboration with UofW, Magna International, and Concordia University. He works broadly on next-generation inverter development, intelligent ETDS for EV application. He is a reviewer of many international journals. His research interests include WBG (SiC and GaN) inverter development, gate driver design, electric vehicle, PMSM drives, multi-level inverters, BMS, and machine learning-based motor control.